Heat Shock alters the distribution and *in vivo* interaction of major nuclear structural proteins – Lamin B with DNA Topoisomerase II, and with nucleic acids

Authors

Marta Rowińska*, Aleksandra Tomczak*, Jadwiga Jabłońska[1], Katarzyna Piekarowicz, Magdalena Machowska and Ryszard Rzepecki[&]

Laboratory of Nuclear Proteins, Faculty of Biotechnology, University of Wroclaw, Wroclaw, Poland, Fryderyk Joliot-Curie Street 14a, 50-383 Wroclaw, Poland www.nuclearproteins.com

[&] Corresponding author: *ryszard.rzepecki@uwr.edu.pl*

*** Joint first author**

[1]present address: Department of Biophysics and Neuroscience, Wroclaw Medical University, Chalubinskiego Street 3A, Wroclaw, Poland

Acknowledgement: Funded by National Centre for Science (NCN) grant Nr 2016/21/B/NZ4/00541

ABSTRACT

Lamins and topoisomerases have been studied as major karyoskeletal proteins since early 80-ties. Today, lamins are thought to be responsible not only for maintenance and structural support of cell nuclei but also involved, directly or indirectly, in regulation of chromatin structure, chromatin distribution, gene expression, splicing, transcription and transport. Topoisomerases are involved in maintenance of chromosomal scaffold and structural functions in cell nuclei and topology of chromatin and DNA, and play an important role in regulation of transcription. They are also necessary in mitosis. For studying lamins and topoisomerase II, *Drosophila melanogaster* model has been used for many years since flies genome contains only single gene coding for B-type lamins (lamin Dm) and single gene coding for A-type lamins (lamin C). Flies have only single gene coding for topoisomerase II (Top2).

We previously reported that lamin Dm (Lam Dm) and topoisomerase II (Top2) bind *in vivo* both DNA and RNA and the properties of both proteins have been modulated by specific phosphorylation on particular sites. Here we report the first part of results of the project focused on the demonstration of the role of lamins and Top2 in the regulation of gene expression and chromatin organization upon heat shock (HS) induction and recovery (R). We demonstrated that heat shock significantly induced specific phosphorylation of lamin Dm at least on S25, which affects lamin properties and distribution. Lam Dm and Top2 were relocated and changed properties including solubility. Both proteins interact with each other directly and indirectly and binding was significantly increased under HS. The relocation of Lam Dm and Top2 was associated with the relocation of chromatin as detected in polyploid third instar larvae nuclei. *In vivo* photocrosslinking and IP (immunoprecipitation) studies indicated a significant increase in binding to chromatin and nucleic acids upon HS induction. The highest binding affinity showed a soluble fraction of lamin Dm and topoisomerase II while the lowest was the insoluble fraction (“nuclear matrix” fraction). All the detected changes in properties and location of proteins returned to “normal” after recovery from heat shock. Based on this data and our preliminary interactome data for lamin Dm and Top2 we believe that both proteins play essential roles in the proper response of fly cells to HS by participation in the rearrangement of protein complexes, also associated with DNA and RNA, chromatin remodelling and proper gene expression regulation.

INTRODUCTION

Lamins and topoisomerase II (Top2) have been considered among the major components of the karyoskeletal structures since early 80-ties studies when commonly used experimental analyses were based on the isolation of nuclear matrix (NM) or chromosomal/nuclear scaffold structures. Importantly, it has been reported, that heat shock (HS) in mammalian cells dramatically enhanced the protein content and affected the composition of NM fractions generated by cell fractionation *in vitro* and sequential extraction [1]. Similar observations were reported for *D. melanogaster* [2]; [3] as well for the formation of the mitotic chromosome scaffold [4]; [5]; [6] and plant nuclear matrix preparations [7]; [8]. To date, the biological/biochemical bases for these well-documented and ubiquitous effects of thermal stress have remained relatively unclear.

Lamins are type V intermediate filament proteins which play a critical role in all nuclear functions in Metazoan starting from mechanical and organizational functions supporting nuclear envelope (NE), nuclear lamina (NL), nuclear pore complexes (NPC), chromatin structure and subnuclear compartmentalization as well as involvement (directly and/or indirectly) in replication, regulation of transcription, splicing, transport as well as a hub or platform for integrating nucleo-cytoplasmic signalling [9]; [10]. Lamins and interacting proteins are also directly involved in the positioning and transport of cell nuclei within cells as well as in mechanical properties of cell nuclei, mechanosensing [11] and mechanotransduction of signals from other parts of the cell and extracellular matrix [12]; [13]. All of these functions lamins play directly or indirectly by forming different protein complexes within different nuclear subcompartments. It has been commonly believed that most of these functions of lamins are regulated by phosphorylation/ dephosphorylation on specific, evolutionally conserved sites, with the help of prolyl-protein isomerase, which affects particular lamin particles polymerization state, location, solubility, interactions with other protein (or protein complexes) and interactions with chromatin components such as histones, non-histone proteins and DNA [14]; [15]; [16]; [17]; [18]; [19].

Typically, Metazoan lamins are divided into two types: A-type lamins which in mammalian somatic cells are represented by lamin A and lamin C proteins that derive from alternatively spliced *LMNA* gene, and B-type lamins, represented by lamin B1 and B2 proteins which are translated in somatic cells and derive from separate *LMNB1* and *LMNB2* genes, respectively. Lamin C variant and lamin B3 (from *LMNB2*) are synthesized in germ line tissues. In *Xenopus* and *Teleostea* fish, there are extra copies of lamin A and lamin B genes, in *C. elegans* there is only a single lamin Ce and in *D. melanogaster*, there are two genes and two lamin proteins: lamin C of A-type and lamin Dm of B-type [20]; [21]. Lamin Dm is present at all stages of fly development while lamin C protein appears in late stage of embryogenesis [56]. The latter has all typical functional protein domains and phosphorylation sites as mammalian lamins homologs. Fly lamin Dm exists as different isoforms depending probably on the phosphorylation pattern.

It has been demonstrated that many different phosphorylation sites can be

modified (for review see [18]), but old ^{32}P labelling studies demonstrated that the average number of phosphorylations per single protein does not exceed 2-3 moieties [16]; [22]; [17]; [23]. In SDS PAGE, Lam Dm fractions migrate at different positions and are named Dm1, Dm2 (so-called interphase forms) and mitotic isoform designated as Dm_{Mit}. Conversion between Dm1 and Dm2 forms has been attributed to S25 phosphorylation [24]. Mitotic, soluble fraction has been thought to arise, similarly to vertebrate lamins by phosphorylation of at least one of two Cdk1-specific sites called "mitotic sites" (for review see [18].

Contradictory to lamins, topoisomerase II structural and organizational roles, especially in interphase cell nuclei, have not been studied so deeply. Previous studies of Top2 focused mostly on its enzymatic role, in the maintenance of proper topology of DNA in chromatin, unwinding during transcription and replication. Above imply Top2 role in the topology of condensing DNA into mitotic chromosomes sister chromatids resolution and structural role in building of mitotic chromosomal scaffold [25]; [26]; [27]; [28]; [29]. *In vivo*, Top2 is essential during mitosis [30]; [31]; [32]; [33]; [34]; [35]; [36] where participation in chromatin condensation [37]; [38]; [39] and in formation of the mitotic chromosome scaffold were implicated [6]; [4]; [5]. It is similarly important in meiosis [40]; [41]; [42]; [43]. As with lamins, a structural role for Top2 in organizing interphase nuclei was previously suggested [44]; [45]; [46]; [47] while the biochemical mechanisms underlining these ubiquitous interactions with RNA and DNA and enrichment in nuclear matrix upon thermal stress are mostly still elucidated. Interestingly, in studies using *Drosophila* tissue culture models, several *in vivo* binding sites for Top2 as well as the induction of new binding sites upon thermal stress were identified. At least some of them are directly related to so-called heat shock loci in *Drosophila* [48].

Our previous studies of Top2 in *Drosophila* confirmed the existence of a heterogeneous population of Top2 fractions in fly tissue culture cells and embryos. We have detected different populations of Top2 with different solubility properties, interactions and phosphorylation status. We reported a correlation of phosphorylation with enzymatic activity of Top2 fractions and reported the C-terminal Top2 domain as phosphorylated and necessary for interactions and regulation of activity [49]. We demonstrated that during mitosis there are two distinct populations of Top2: one associated with mitotic chromosomes and the second dispersed through the cell. We also demonstrated, that Top2 binds to DNA and RNA *in vivo* during interphase and mitosis and the critical region of binding domain lays within 200 amino acid residues of the C-terminal Top2 protein [49].

In the case of fly lamins we previously discovered that lamin Dm does bind *in vivo* DNA and RNA during interphase but not during mitosis while lamin C did not bind to nucleic acids at all in our tests [50]. Fly lamins similarly to mammalian lamins undergo specific phosphorylation/ dephosphorylation during the cell cycle *in vivo* [22]; [18]. Analyses of the function of single phosphorylation sites in lamins, using pseudo-phosphorylation mutants demonstrated that single phosphorylation on S37 (Cdk1-N-terminal site) on lamin C induces the solubility while for lamin Dm both N-terminal and

C-terminal Cdk1 mitotic sites and to the lesser extent also S25 increased solubility [17]. All single pseudo-phosphorylation mutants tested, except lamin C S37E, did bind to decondensed chromatin in an *in vitro Xenopus* assembly system. Expression of the mutants in insect Kc cell line and HeLa cells resulted in atypical distribution (partly cytoplasmic, intra-nuclear diffused, decreased presence at NL) for lamin Dm single mutants: S45E, T435E and to the lesser extent S595E which indicates the correlation between phosphorylation, solubility, intracellular distribution, and DNA/chromatin binding. Thus supporting the thesis of lamins properties being dependent on phosphorylation pattern.

Since lamins and Top2 have been identified as major karyoskeletal proteins, with an enhanced presence in NM upon stress induction, which has been correlated with the induction of new, heat shock-specific binding on DNA, we decided to look closely into the molecular mechanisms regulating lamins and Top2 interactions upon stress induction. We analyzed the effect of thermal stress on selected, most important properties and interaction of lamins, Top2 and other important nuclear proteins focusing on their subcellular distribution, solubility, phosphorylation, interactions, chromatin binding and their modulations upon reversible thermal stress induction.

MATERIALS AND METHODS

Antibodies

Affinity-purified rabbit anti-lamin Dm and domain-specific rabbit anti-Top2 antibodies used in this study have been previously described [49]. Guinea-pig anti-LBR was a generous gift from Georg Krohne, University of Würzburg, Germany [51]. Mouse monoclonal antibodies ADL67.10, ADL84.12, and LC28.26 were from Developmental Studies Hybridoma Bank (DSHB). Mouse and rabbit anti-α-tubulin were from DSHB (clone 12G10) and ThermoFisher (#PA5-29444), respectively. The monoclonal rat anti-Hsp70 (heat shock protein 70 kDa) antibody (NBP2-59342) and rabbit polyclonal antibody against histone deacetylase I (HDAC1; #NB500-124), were from Novus Biologicals. The rabbit polyclonal antibody anti-Hsf (heat shock factor) was custom-made for us by ThermoScientific. Additional immunofluorescence staining was performed with the rat anti-Hsp90 (heat shock protein 90 kDa; #ab13494) and rabbit anti-Pol2PS5 (RNA polymerase II, phosphorylated at Ser5; #ab5131) both from Abcam, and rabbit anti-HP1 (heterochromatin protein 1; #NB110-40623) from Novus Biologicals.

The secondary antibodies were from Jackson ImmunoResearch. The HRP conjugated antibodies anti-mouse (#715-035-151), -rabbit (#111-035-144), and –rat (#712-035-153) were used to visualize antigens on membranes after immunoblotting. Secondary antibodies anti-mouse used for immunofluorescence were conjugated with TRITC or DyLight649 (#715-025-151, #715-495-150). Antibodies anti-rat were coupled to TRITC (#712-025-153), while antibodies against rabbit were conjugated with Alexa488 (#711-545-152).

Drosophila melanogaster embryos and cell cultures

D. melanogaster Oregon R-P2 strain (RRID:BDSC_2376) came from Bloominghton Drosophila Stock Center, Bloomington, USA (NIH P40OD018537). Embryos were collected in special egg-laying cages. Flies were transferred from standard medium (6,25% w/v corn grits, 3,13% w/v corn flour, 6,25% w/v sugar, 12,5% w/v yeast and 0,5% w/v bacteriological agar) to cages with embryo assembly medium (20 ml apple juice, 10 ml cherry syrup, 10 ml water and 2,5 g sugar, 1,6 g bacteriological agar, coated with yeast paste). The flies were allowed to lay embryos for 11 hours and then a 1-hour heat shock in 37°C was performed. The analyzed embryos were in the age range from 1 hour to 12 hours old. After induction of heat shock, the embryos were rinsed with water from the medium to special strainers with a nylon filtration fabric NITEX (40 µm). The chemical dechorionation procedure was carried out successively using 5% sodium hypochlorite. Then embryos were washed with a washing buffer (5 mM NaCl, 20 mM Tris-Cl pH 7,5, and freshly added protease and phosphatase inhibitors).

Kc cells (ECACC #90070550) and S2 cells (Drosophila Genomics Resource Center; Stock 6; https://dgrc.bio.indiana.edu//stock/6; RRID:CVCL_TZ72, a kind gift from Department of Cytobiochemistry, University of Wroclaw, Poland) were cultured in Schneider's Drosophila Medium (Gibco #21720024), complemented with 10% fetal

bovine serum (Sigma #7524) and 1% antibiotic-antimycotic (Gibco #15240062) at 23°C (N) without additional CO_2. Cells were plated on a 10 cm culture dish 24 hours before each experiment. Cells' collection was performed by gently scratching cells from culture plates and pelleting by centrifugation.

Cell pellets were re-suspended in the Laemmli loading buffer and heated at 95°C for 10 minutes before WB analysis. For heat shock induction, material (embryos, larvae and cells) were shifted to 37°C and maintained at this temperature for 1h (or a certain amount of time as indicated in the text). Recovery (R) was initiated by a return to 23°C for an additional: 6, 24, 48, 72 h or 96h.

Western Blot analysis

Proteins were separated on polyacrylamide gels (in the concentration in the range between 7% and 12% depending on the experiment) according to Laemmli[52] and then electrophoretically transferred to nitrocellulose membranes according to Harlow and Lane, 1988 [53] (0,45 µm; Amersham Protran) using Bio-Rad`s Mini Trans-Blot Cell set. To estimate protein sizes prestained protein ladder from ThermoFisher (#26616) was used. After 1h of blocking with 5% non-fat milk in PBST (PBS, 0,075% Tween-20), the membrane was incubated with primary antibodies over night at 4°C then washed three times with PBST and incubated with secondary antibodies conjugated with HRP for 1,5 h at RT. Proteins were detected by using SuperSignal™ West Pico PLUS Chemiluminescent Substrate (ThermoFisher #34580) or Clarity Western ECL Substrate (Bio-Rad #1705061). Images were acquired and quantified using the ChemiDoc MP Imaging System (Bio-Rad) and the software Image Lab V5.2 (Bio-Rad).

When reactivity was visualized colourimetrically, calf alkaline phosphatase-conjugated goat anti-IgGs antibodies and/or horseradish peroxidase coupled with donkey anti-IgGs with proper single or both substrates.

Immunofluorescence

Cells were cultured on gelatin-coated cover slides for 24 h and heat shocked if necessary before fixation. Cells were fixed with 4% paraformaldehyde, permeabilized with 0,5% Triton X-100 in PBS solution and blocked with 5% FBS in PBS solution. Cells and embryos have been processed as described previously [54]; [50].

Before fixation, the embryos were subjected to chemical dechorionation (3 min, 5% sodium hypochlorite) and then rinsed with water. Embryos were fixed with 4% PFA (300 µl) with heptane (1 ml) at RT for 20 min. After incubation fixative phase was replaced with 1 ml of methanol, washed twice with PBS and then hydrated with PBS with 0,1% Triton X-100 for 30 min at RT. Permeabilization was carried out for 30 min in PBS with 0,5% Triton X-100 at RT with stirring. Finally, the embryos were washed with PBS and stained as described below.

Subsequently, cells and embryos were stained with primary antibodies overnight at 4°C and after that secondary antibodies at room temperature (RT) for 1,5 h.

PLA staining with Duolink PLA Multicolor Reagent Pack (Sigma-Aldrich, #DUO96000) was performed according to manufacturer instructions. Primary antibody

incubation was performed for 16 hours at 4°C, slides were washed with PBS, and incubated in secondary antibodies PBS solution for 1,5 h at RT. Slides were washed with PBS and mounted with VECTASHIELD medium with DAPI. PLA staining has been performed on Kc cells and third-instar larvae (smears were prepared from larvae and processed in the same way as cells). Prepared samples were stained according to manufacturer protocol. Microscope images were collected with a Leica SP8 confocal microscope and adjusted with a Fiji image processing package.

Solubility assay

Kc cells and S2 cells

Cells were plated 24 hours before the experiment (2,5 x 10^6 cells/ml). After heat shock induction cells were scratched from plates, shifted to 15 ml tubes, and collected by centrifugation at 500 x g for 5 minutes and washed with PBS. Cell pellets have been suspended in extraction buffer (5 mM $MgCl_2$, 50 mM NaCl, 50 mM Tris-HCl pH 7,5, 250 mM sucrose, 0,1 m EDTA, 1% Triton X-100 and freshly added protease and phosphate inhibitors). After mechanical homogenization, the prepared lysate was incubated for 20 minutes on ice (control - the fraction of cell lysate was collected before further steps). Then centrifugation was performed (10 000 x g, 10 min, 4°C) and the supernatant was collected (fraction of proteins soluble in 50 mM NaCl), the pellet was resuspended in the same buffer as above with 150 mM NaCl and incubated for 20 min on ice, then centrifuged and the next fraction was collected (soluble in 150 mM NaCl). Further, it has proceeded with a 500 mM NaCl extraction buffer. Collected samples were boiled in a denaturing buffer (5% DTT and 40 mM DTT) for 10 min at 96°C and prepared for SDS-PAGE in the standard Laemmli loading buffer.

Embryos

Collected and washed embryos were suspended in the extraction buffer (the same as in the cells section) in the proportion of 25 mg of embryos to 125 µl of the buffer. The next steps of extraction were carried out analogously to those described above.

RNA extraction and first-strand cDNA synthesis

Semi-adherent Kc cells were plated at the density of 2,5 x 10^6 cells/ml of Schneider medium on the 6 cm cell culture plate. (In a total of 1,5 x 10^7 cells). After 24 h medium was aspirated and cells were washed once gently with PBS. Then the first - lysis buffer from the Universal RNA Purification Kit (Eurx) was added and all further procedures were performed following the manufacturer's protocol. DNAse I (Eurx) treatment was performed. The RNA concentration and purity were evaluated with NanoPhotometer® N60 (IMPLEN). RNA samples with an absorbance ratio of A 260/280 over 2,2 and A 260/230 over 2,2 were used for further analysis. The quality of the RNA samples was verified on 1 % native gel electrophoresis.

Single-stranded cDNA was synthesized from 2 µg of total RNA in a final volume of 10 µL. For this purpose, the Maxima First Strand cDNA Synthesis Kit for RT-qPCR

(Thermo Scientific) was used and the manufacturer's instructions were followed. cDNA was stored at −20°C for future use.

RNA extractions and cDNA synthesis from all samples were performed for three biological replicates.

Real-time quantitative PCR analysis

qPCR was performed using Power SYBR Green Master Mix (Applied Biosystems). All reactions were performed under the following conditions: 1) UDG activation 50°C for 2 min, 2) Dual-Lock DNA polymerase 95°C for 2 min, 3) 40 cycles of denature and anneal/extend 95°C for 1 s and 60°C for 30 s. The specificity of the reaction was verified by melting curve analysis and agarose electrophoresis of PCR product. All qPCR experiments were performed using QuantStudio™ 5 Real-Time PCR System. See primer sequences: Figure 2 – figure supplement 2.

For each well of the plate, the threshold crossing value (Ct) was calculated by the thermocycler manufacturer software (Quant Studio Design and Analysis). Further analyses were carried out based on the comparative Ct method. Values were normalized to the most stable gene in the dataset. Statistics between N and HS groups were calculated using t-student tests.

Photo-crosslinking and ^{32}P-end-labeling of co-immunoprecipitated nucleic acid

BrdU incorporation in Kc cells

For routine 5-bromo-2-deoxyuridine (BrdU) incorporation, quantified with an anti-BrdU monoclonal antibody as previously described [50], 200 ml of exponentially growing cells (1,2-1,8 x 10^6 cells/ml) were made 20 μM BrdU and maintained in culture for an additional 26-27 hours [50]. 5-bromo-2-deoxycytidine (BrdC) incorporation was achieved similarly.

Cell fractionation of ^{32}P labelled and UV cross-linked cells

Cell fractionation was performed according to [49]; see also [46]. In brief, cells were harvested by centrifugation and washed with PBS. Lysates were prepared using a Dounce homogenizer, the homogenates were filtered and centrifuged (10000 x g, 10 min) to obtain fractions marked as P-10 and S-10 (pellet and supernatant, respectively). The obtained supernatant was then centrifuged (13000 x g, 60 min) to obtain P-130 fraction.

In vivo photo-crosslinking

In vivo photo-crosslinking was performed as described previously [50]; [49]. The hand-held lamp (UVGL-58, UVP Inc., San Gabriel, CA) emitting 366 nm light was used. All quantities refer to 200 ml of cell culture starting material. In experiments with distamycin, cells were grown, harvested, washed and re-suspended in 8 ml of PBS, exactly as described before. However, before illumination, cell suspensions were made

with 50 µM distamycin A3 and/or chromomycin (Sigma). After antibiotic addition, cell suspensions were incubated for 30 min at RT and then subjected to illumination with 366 nm light as described above.

Immunoprecipitation and ^{32}P-end-labeling of co-immunoprecipitated nucleic acid

The entire procedure has been described previously [50]; [49]. After *in vivo* photocrosslinking, cells were lysed for cell fractionation or lysed directly and denatured by the addition of SDS and DTT (final concentrations of 5% and 20 mM, respectively); after the addition of SDS and DTT, samples were boiled for 10 min. Typically, about 6 x 10^8 cells were harvested, resuspended in 1,5 ml PBS, lysed and either denatured immediately or fractionated and then denatured by the addition of a solution containing 10% SDS and 40 mM DTT. Whole-cell lysates and/or subcellular fractions prepared in this way were stored at -20°C until use. Samples, each derived from about 1,5 x 10^7 cells, were thawed by boiling for 10 min, cooled to room temperature and trichloroacetic acid (TCA) was added to a final concentration of 10%. Samples were then incubated for 10 minutes at room temperature and precipitated proteins were collected by centrifugation, also at room temperature, for 10 min at 10,000 x g. The supernatant was discarded, 5 µl of 1,5 M Tris-HCl pH 8,8 was added to the protein pellet and the pellet was dissolved in 200 µl of a solution containing 20 mM Tris-HCl pH 8, 150 mM NaCl, 0,1 % Triton X-100 and 0,02 % SDS (Buffer IPA). Immediately before use, Buffer IPA was supplemented that the final concentration was 2,5 mM $CaCl_2$, 0,5 mM PMSF, 1 mM TPCK, 1 mM TLCK, 1 µg/ml leupeptin and 1 µg/ml pepstatin. Unless indicated otherwise, 5 µl of micrococcal nuclease (680 µg/ml; Boerhinger) was then added and samples were incubated for 60 minutes at 37°C.

Immunoprecipitation was performed as modified by Rzepecki et al. Briefly, for this purpose Protein A-Sepharose (Pharmacia, Piscataway, NJ) conjugated with antibodies was used (2-4 µg of purified IgG was used per 50 µl beads and incubated for 90 min at 37°C). The supernatant was successively centrifuged and the buffer with unbound antibodies was discarded. Incubation of the prepared beads with the prepared lysates was carried out for 90 min at 37°C. The beads with IgG and antigen bound (immunoprecipitate) were recovered by centrifugation, and washed three times with 350-µl each of Buffer IPB followed by three identical washes with Buffer IPA [50], [55].

Nucleases and nuclease digestion

Nucleases and nuclease digestions were carried out exactly as described previously [50]. To study the sensitivity of ^{32}P-labeled nucleic acid photo-crosslinked to Top2, nuclease digestions were performed for 30 min at 37°C with final concentrations of 66 µg/ml of DNase I and 60 µg/ml of RNase A. All nucleases digestions were performed in a solution containing 20 mM Tris-HCl pH 8, 150 mM NaCl, 0,1% (v/v) Triton X-100 and 0,02% (w/v) SDS (Buffer IPA) supplemented with 5 mM $MgCl_2$ and 2,5 mM $CaCl_2$.

Quantification by scanning densitometry

Unless stated otherwise, immunoblots and autoradiograms (or PhosphorImager scans) were quantified using an LKB Mltrascan XL laser densitometer (LKB Instruments Inc., Gaithersburg, MD).

PFA-crosslinking and co-immunoprecipitation

Cells collection and crosslinking

HS induction and cell collection were performed in the same manner as for the solubility assay. Pelleted cells (25 x 10^6) were resuspended in 2 ml of cross-linking reagent (1% paraformaldehydu) and incubated for 7 min with gentle rotation on a rotary agitator at RT. After incubation cells were immediately centrifuged for 3 min, 1000 x g at RT. Pelleted cells were resuspended in 1 ml of 125 mM glycine solution (to quench the PFA and terminate the cross-linking process) and incubated on a rotary for 5 min and then centrifuged at 4°C.

Next, cells were washed with cold PBS with proteases and phosphatases inhibitors, centrifuged, and resuspended in lysis buffer (50 mM Tris-Cl pH7,5; 150 mM NaCl, 1 mM EDTA, 1% Triton X-100, 0,1% SDS, Halt Protease and Phosphatase Inhibitor Cocktail from ThermoScientific) and transferred to 1,5 ml tubes. Mechanical homogenization was performed with plastic pestles with the following incubation for 20 min on ice. The prepared lysate was sonicated (Bandelin Sonoplus Mini 20) for 25 minutes at 90% amplitude with a pulse (30 sec ON-OFF cycles). The sonication has been optimized to obtain a homogenous trace of DNA <500 bp with no protein loss. After sonication lysate was centrifuged at 8000 x g, 10 min at 4°C. The supernatant was taken for further steps.

Co-immunoprecipitation

According to the manufacturer manual, 25 µl of the Pierce Protein A/G Magnetic Beads (ThermoScientific # 88802) per sample was used. Initially, 200 µl of cell lysate with 10 µg of primary antibody (anti-lamDm, anti-Top2) were rotated for 1,5 h at RT (volume adjusted to 500 µl with lysis buffer). Then the antibody-lysate mixture was transferred to previously washed beads and incubated for 1 h at RT with rotating. The beads were collected with a magnetic stand (ThermoFisher #CS15000) between each washing step. Before the first wash, the flow-through fraction (excess of unbound antibodies and lysate) was collected for further analysis. Elution was performed by adding 100 µl of Laemmli buffer and heating samples for 10 min at 96°C. After cooling, the supernatant was collected.

The negative control in the experiment was samples treated identically, except the antibodies – as an isotype control normal polyclonal rabbit IgG was used (R&D Systems, #AB-105-C).

The 10 µl of each sample was loaded onto polyacrylamide gel together with corresponding controls (input, negative control, and flow-through fractions) and proteins were detected by immunoblotting using primary antibodies (anti-lamDm, anti-Top2, anti-

LC28.26) followed by HRP-conjugated anti-rabbit or anti-mouse IgG (described in *Antibodies* section).

Quantitative densitometry analysis of protein level and solubility assay

Bands detected by immunoblotting were quantified using Bio-Rad Image Lab with the use of the volume tools. The area of the stained band was marked with a rectangle (the areas were identical for each band on the membrane). The mean value of intensity was acquired from the generated analysis table.

For protein level estimation the signal intensity value for a protein of interest was normalized to the signal intensity from housekeeping proteins (e.g. tubulin).

For the solubility assay, each of the successive fractions (50 mM, 150 mM and 500 mM) was plotted (Figure 5A, B and Supplementary Figure 5B) as the percentage of output lysate which was considered as 100% for each replicate. The statistic shows the comparison of normal versus heat shock conditions for each fraction. For Supplementary Figure 4 and Supplementary Figure 5C the acquired signal intensity value presented on the graph was normalized to the mean value of all intensity values for an examined fraction. Only the N and HS values within a fraction were compared with each other.

Statistical analysis and data presentation

Statistics (Fisher's exact test and t-test unless indicated otherwise in the text) were calculated using Microsoft Excel. Quantified data were plotted using GraphPad Prism 8.0. The details of experimental replicates and statistical analysis are mentioned in the corresponding figure legends. Independent experiments mentioned in the figure legends indicate biological replicates.

Data availability

All data associated with this manuscript have been deposited on the Faculty of Biotechnology, University of Wrocław server. Please contact the Authors for login and password details.

RESULTS

Induction of heat shock and recovery in *Drosophila melanogaster* tissue culture cells and embryos

For this study, we have chosen a fruit fly cell culture model system based on Kc and S2 cells and whenever possible we have also tested embryos and larvae at desired stages. Lamin Dm is present in both cell types while lamin C is present only in Kc cells. First we tested the conditions and reversibility of thermal stress induction (heat shock, HS) and recovery time (R) using inducible Hsp70 protein as an HS marker. Figures 1A and 1B demonstrate that HS induction can be easily detected and followed by IF in Kc and S2 cells and Panel C illustrates the time frame of Hsp70 protein induction, detected by WB in Kc and S2 cells respectively. Panel D illustrates the level of selected marker HS inducible genes including *Hsp70*. Figure 1 - Figure supplement 1 demonstrates Hsp70 induction and recovery in embryos using IF. Altogether it is evident that the HS effect in all samples is typical and fully reversible. Based on the remaining levels of Hsp70 proteins in WB experiments similar to those demonstrated in Fig1C we have chosen 48 and 72 hours as best for recovery time for S2 and Kc cells respectively while as the optimal time for HS induction, we set 1h. Since HS affects the expression of many genes [57], [58] we have tested several genes or their combinations as references for RT-qPCR analyses for normal (N) and heat shock (HS) conditions. Based on our analyses (Figure 2 – figure supplement 1A) the most stable seems to be ribosomal RNAs, actin5C and tubulin84B. According to geNorm analyses (Figure 2 – figure supplement 1B) these genes are also detected as having the most stable transcripts comparing HS versus N.

Considering above we have chosen as references for RT-qPCR 18S/28S ribosomal RNA, actin5C and tubulin84B. Please note that we have detected the transcript for lamin C in S2 cells, but this signal was visible only after at least 7 cycles after than in Kc cells transcript and on WB we did not detect lamin C protein in S2 cells (Figure 2 – figure supplement 1A).

Quantitative analyses of transcripts for lamin Dm, lamin C, Top2 and Hsf using RT-qPCR indicated that their transcript levels do not change significantly after heat shock but for lamins and Top2 we observed a tendency for decrease while for Hsf increase in level in both cell lines (Figure 2A). Comparison of the induction of typical HS genes revealed that stress induction of their transcript is slightly lower in S2 than in Kc cells (Figure 2B).

Heat shock affects phosphorylation level of lamin Dm but does not affect total protein level

We tested the level of selected proteins during the HS induction and recovery in Kc and S2 cells using western blotting. For Kc cells, we have not observed any statistically significant changes in the level of Top2, both lamins, HDAC1 and Hsf (Figure 2C). Please note the modified mobility of the Hsf protein band (Figure 2C and 2D) which is phosphorylated upon HS [59]. Interestingly, HS induces changes in proportions between lamin Dm isoforms-induces the conversion of lamin Dm1 (lower band) into Dm2 isoform as seen in blots stained with rabbit polyclonal antibodies anti lamin Dm (Figure 2C, D; see also Figure 6G). Since the effect is reversible together with HS reversion we suggest it is HS-specific lamin modification. It has been reported previously that fly lamin conversion from Dm1 into Dm2 is correlated with phosphorylation of N-terminal fragment and at least one phosphosite was identified as S25 [24]. To confirm the conversion of lamin Dm upon HS induction we have used monoclonal antibodies ADL84 specific for N-terminal lamin Dm fragment which recognize only lamin Dm when S25 is not phosphorylated. Please note that phosphorylation of S25 abolishes recognition by these antibodies [24]; see also [22]. Using this antibody for western blotting we identified a single band and its optical density decreases upon HS and returns to normal level upon recovery (Figure 2C). Densitometry analyses (illustrated by diagram in 2C; see also Figure 3B) of this staining indicated that the change is statistically significant. Similar analyses performed on S2 cells using WB are illustrated in Figure 2D and associated diagrams from densitometry analyses. S2 cells differ in stress response from Kc cells since we detected a significant increase in Top2 level, less significant conversion of lamin Dm into Dm2 form (S25 specific phosphorylation detected *via* decreased intensity of ADL84 antibodies staining), slightly increased levels of Hsf and HDAC1 proteins (see also Figure 3C).

Since phosphorylation of lamins can affect the properties and interactions of lamins we looked into the phosphorylation of lamin Dm more deeply. Immunofluorescence analyses using ADL84 monoclonal antibodies indicate the partial disappearance of the signal for non-phosphorylated (at the S25) lamin Dm upon HS induction (Figure 3A). Western blot analyses of Kc cells illustrate the conversion of lamin Dm1 fraction into lamin Dm2 fraction – the disappearance of signal from ADL84 antibodies and change in the proportion of lamin Dm isoform in polyclonal Ab staining (Figure 3B). Densitometry of western blotting confirms that the changes are statistically significant. A similar experiment on S2 cells also confirmed the conversion of lamin Dm1 into lamin Dm2 by S25 phosphorylation (Figure 3C) and its statistical significance.

Stress changes reversibly the distribution of Top2 and chromatin but does not affect detectably distribution of lamins.

Since thermal stress induces new *in vivo* binding sites for Top2 on chromatin and affects the compositions of isolated karyoskeletal structures (nuclear matrix/chromosomal scaffold) [60], [61] we looked into the distribution of Top2 protein upon thermal stress and recovery (Figure 4). Immunofluorescence analyses of Kc cells

for Top2, Hsp70 and lamin Dm indicated relocation of Top2 upon HS induction from intranuclear mostly homogenous distribution into lateral distribution with frequently observed spherical Top2 bodies/granules (Figure 4A, (arrowheads)). For lamin Dm staining we did not observe any detectable changes in distribution but detected lower fluorescence intensity (Figure 4A). No changes in the distribution of lamin C were observed (Figure 4C). In embryos, we also detected relocation of Top2 into the peripheral, NL-related location with a general decrease of the signal which was reversible (Figure 4B and D). This was confirmed by optical density scanning demonstrating intra-nuclear signal disappearance upon HS induction (Figure 4F). The effect was reversible. Quantification data indicate the statistical significance of the redistribution of Top2 into nuclear lamina fraction (Figure 4E). To test if redistribution of Top2 is correlated with redistribution of DNA we choose third instar larvae nuclei which are poliploidic and have nicely detected chromatin. Figure 4H demonstrated the relocation of chromatin to nuclear lamina regions which was calculated to be statistically significant (Figure 4G). For lamin Dm, we detected in Kc cells a decrease of the signal while in embryos and especially in larval nuclei we detected less “diffuse” staining for lamin and increased intensity of the signal at the NL (e.g. Figure 4Fand 4H respectively). Please also look at the supplementary material with additional immunofluorescence staining (Figure 4 – figure supplement 1 and 2 for Kc cells and embryos, respectively).

Since HS affects the distribution of Top2, lamin and chromatin we tested the solubility of lamins, Top2 and other nuclear proteins in Kc cells, S2 cells and embryos as well (Figure 5 and Figure 5 – figure supplement 1 and 2) with 50 mM, 150 mM and 0,5 M NaCl in buffer comparing normal condition and heat shock induction.

We observed significant changes in solubility of lamin Dm – increased level of protein in high salt extracts in Kc cells, decreased soluble fraction of Top2 protein (50 mM NaCl), decreased soluble fraction of HDAC1 and increased level of high salt (0,5 M NaCl) fraction of protein. Similar results were obtained for Hsf protein – significant decrease in the soluble fraction of protein and an increase in high salt fraction (Figure 5A and 5C, and Figure 5 – figure supplement 1). Similar experiments in S2 cells showed for lamin Dm significant changes only in medium salt concentrations (less soluble; 150 mM NaCl) fraction, no significant changes in Top2, but changes in HDAC1 and Hsf solubility-decrease in soluble fraction and increase in high salt fraction (Figure 5B and 5D). Similar data were also obtained for embryos (Figure 5 – figure supplement 1).

Lamin Dm interacts with Topoisomerase II directly and through adjacent chromatin DNA regions and interactions are increased during heat shock

In earlier studies on Top2 and lamins, we confirmed that both proteins bind to chromatin and nucleic acids *in vitro* and *in vivo* [49] and we also got preliminary data suggesting their possible interactions. We decided to test whether these proteins interact with each other. Immunofluorescence analyses of the distribution of lamin Dm and Top2 demonstrate that the most of the proteins are located separately within typical

cell nuclei with lamin Dm at the nuclear lamina and Top2 more or less evenly dispersed within nuclear interior/entire cell nuclei (Figure 6A see also Figure 4) which is correct for cell in cell culture and in embryos and larvae. Panel 6A demonstrates merged staining for lamin Dm and Top2 in larval cell nuclei: polyploid (both left and top right picture) and diploid (bottom right). Panel B demonstrates colocalization of lamin Dm and Top2 in Kc cells (top series) and polytenic nuclei of salivary gland cells of the third instar larvae (bottom series) using proximity ligation assay technique (PLA) using anti lamin Dm monoclonal ADL67 antibody and affinity purified anti Top2 antibodies. Panel C demonstrates magnifications of a single Z-section from movies (see also Figure 6 – movie 1) from IF analyses of PLA showing the interaction of Lam and Top2 in polytene chromosome cell nuclei. Please note that the colocalization signal was detected not only at the contact of chromatin with nuclear lamina but also on the surface of polytenic chromosomes inside cell nuclei.

Please also look at the supplementary material with corresponding movies (Figure 6 – movie 1).

We performed an immunoprecipitation experiment for lamin Dm using embryo extracts and anti-lamin Dm, affinity purified, rabbit polyclonal antibodies and detected lamin Dm and Top2 proteins with ADL67 monoclonal and affinity-purified polyclonal antibodies for lamin Dm and Top2, respectively, using different amounts of extract loaded into each reaction. The result shown in Figure 6D demonstrates the co-immunoprecipitation of Top2 protein with lamin Dm and the correlation of the amount of bound lamin Dm and Top2 protein with the amount of extract loaded. Figure 6E demonstrates co-immunoprecipitation of Top2 with lamin Dm from extracts from Kc cells (under native conditions) with additional S1 nuclease treatment (on beads) demonstrating the interaction is predominantly not nucleic acid dependent. Immunoprecipitation experiment performed under denaturing conditions on Kc cells (Figure 6F, IP anti-Lam Dm) (see also Figure 6 – figure supplement 1 for S2 cells) indicated that lamin Dm interacts with Top2 during normal conditions and after heat shock induction. Please note stronger Top2 band co-precipitating with lamin Dm during HS and modified proportion of lamin Dm fractions: Dm1 and Dm2 upon heat shock (Figure 6G). Similarly, lamin Dm co-precipitates with Top2 and the intensity of lamin bands is stronger upon HS compared to normal conditions (Figure 6F, co-IP anti Top2).

Therefore we performed PLA colocalization studies comparing the normal conditions and thermal stress induction (Figure 6H, I, J). We indicated that heat shock induction significantly increased the colocalization between lamin Dm and Top2 in Kc cells (Figure 6H). Quantification of the signal indicates a significant increase in detected *foci* per cell nucleus upon stress induction in Kc cells (Figure 6I). Figure 6J demonstrates the typical amount of *foci* detected in diploid cell nuclei and polytenic nuclei in third-instar larvae preparations.

To get better insight into the lamin Dm-Top2 interactions with chromatin, nucleic acids and themselves we decided to use our previously used technique of *in vivo* BrdU labelling, *in vivo* photocrosslinking, immunoprecipitation and 32-P labelling of nucleic acids bound to protein followed by WB and Phosphoimager analyses. The results of the

experiment are demonstrated in Figure 7. IP for lamin Dm in such experiment indicated co-immunoprecipitation of Top2 protein and association of labelled nucleic acids with Top2 (Figure 7A, nuclease -) while additional treatment with nuclease to cleave off nucleic acid decreased the co-IP for Top2 which was correlated with labelled nucleic acid disappearance (Figure 7A nuclease +). Control experiments with IP anti-Top2 and IP anti lamin Dm with additional nuclease treatment (+) or not (-) (Figure 7B) indicated that nuclease treatment simultaneously decreases the co-IP of both proteins in *in vivo* crosslinking procedure suggesting that at least some population of lamin Dm and Top2 has been crosslinked *in vivo* on nucleic acid (chromatin?) next to each other. Previous experiments with native IP and nuclease (Figure 6E) indicated that only a fraction of co-IP was dependent on nucleic acids. Therefore we assume that both protein-protein (or protein complex-protein complex) and protein-nucleic acid-protein type complexes can exist for lamin Dm interaction with Top2. When we looked into the analyses of nucleic acids associated with Top2 and lamin Dm and the effect of thermal stress on the specificity of binding (Figure 7C) using an *in vivo* photolabelling procedure we detected preferential binding to DNA during normal conditions for both proteins and increase in proportion of binding to RNA upon heat shock induction. It is also visible that the radioactive label associated with both proteins is less sensitive for nucleic acid digestion compared to normal conditions. Since HS increased the amount of lamin Dm and Top2 in insoluble, karyoskeletal fraction (nuclear matrix, chromosomal scaffold), and HS affected the solubility of proteins in our experiments, we tested the ability to bind nucleic acids of total fraction of particular protein and compare to soluble or insoluble, karyoskeletal fraction (Figure 7D). We discovered that lamin Dm highly bound to the nucleic fraction appeared to be a soluble fraction while the least was the “insoluble” fraction of lamin Dm. For Top2, a soluble fraction of protein was the most efficiently bound to nucleic acid while an insoluble fraction was the least associated with nucleic acids. When we tested the overall efficiency of nucleic acid binding for lamin Dm and Top2 comparing normal conditions, stress induction and recovery we detected that heat shock dramatically increases the association of Top2 with nucleic acids and the effect is reversible upon recovery (Figure 7E). For lamin Dm, we observed an increase in the efficiency of nucleic acid binding upon stress induction and a decrease of binding upon recovery. We also decided to test the effect of distamycin (an antibiotic frequently used [62]–[64] for probing Top2 [65] and lamin interactions with chromatin [66]; see also [50]; [49]) in our current *in vivo* photocrosslinking studies (Figure 7F). Comparison between normal and heat shock confirmed a stronger association of both proteins with nucleic acids during heat shock induction and as expected indicated the effect of distamycin on decreasing the binding of both proteins with DNA visibly but not completely. This suggests high heterogeneity of the protein- DNA interactions since distamycin has a preference for AT-rich sequences. Figure 7G demonstrates the control experiment that none of the experimental procedures of BrdU labelling *in vivo* photocrosslinking induces a heat shock effect in Kc cells.

DISCUSSION

Drosophila melanogaster tissues, especially salivary glands with polytenic nuclei, together with tissue cultured cells such as Kc and S2 have been widely used as an important model for studies of cell nuclei functions and chromatin structure. The initial attempts at resolving the architecture of skeletal structures of the cell nucleus as well as chromatin composition and organization within karyoskeletal structures, (when the terms either of nuclear matrix/chromosomal scaffold, nuclear lamina or SAR/MAR DNA have been introduced) have been also performed very frequently on the fruit fly model. The fly model has also been useful in the identification of lamins and Top2 as major karyoskeletal and nuclear matrix/chromosomal scaffold proteins as well as their content in karyoskeletal fractions, and their properties depend on preparation methods and condition of initial biological material used for preparation. For example, pretreatment of fly material at 37°C or mammalian material at 42°C (heat shock) resulted in a higher amount of lamins and Top2 in prepared karyoskeletal structures while RNAse treatment along the procedure resulted in the almost complete loss of karyoskeletal proteins including lamins and Top2 from such preparations [67]; [3]; [2]; [68]. Similar differences in protein composition of NM/NS prepared by different methods have been also detected in plants [7], [8]. Our and others papers focused on the role and properties of lamins and Top2 in the fly model demonstrated *in vivo* interactions of lamins and Top2 with both DNA and RNA and that they interact mostly with AT-reach regions of DNA. They exist in cells in different complexes with different posttranslational modifications which affect their properties of nucleic acid binding, nuclear import for lamins and activity for Top2 [1]. Therefore it was natural continuation for us to approach the question of the role of lamins and Top2 in the regulation of chromatin structure, gene expression and chromatin binding in normal conditions and during heat shock. Especially that HS rearranges global gene expression profile upon induction [2]. For that purpose, we used well known, also for us, fruit fly model system of Kc and S2 cells and if necessary fly tissues from embryos and larvae. Both cell lines have been widely used for mapping of *in vivo* Top2 binding sites at normal conditions and during heat shock by many laboratories and there have been many reports on the mapping of several, heat shock-induced Top2 binding sites [65]; [5]; [14]; [60]; [46].

For monitoring of heat shock effect induction we have selected an inducible form of Hsp70 protein for WB and IF studies and a set of inducible heat shock protein-coding genes for RT-qPCR. We have selected the HS induction time at 60 minutes just to allow for efficient transcription and translation into a protein of a first round of heat shock inducible genes which products should efficiently undertake transcription of secondary heat shock inducible genes with associated changes in chromatin structure and protein complexes associated with them. We have always tested the viability of cells during the experiment and recovery and found that the vast majority of cells fully recovered from the HS as indicated by Hsp70 (WB and IF). Since the transcripts of typical reference housekeeping genes were not fully stable during HS and recovery, we selected a set of

four reference transcripts for RT-qPCR studies (18S/28S RNA, actin 5C and tubulin 84B). Interestingly, the level of induction of selected HSP genes is lower in S2 than in Kc cells. Real-time PCR studies demonstrated no statistically significant changes in transcript levels (changes less than 2x) for lamins, Top2, and Hsf. This nicely correlates with stable protein levels for lamins, Top2 and HSF during normal condition, HS and recovery.

WB analyses demonstrated reduced mobility of Hsf protein under HS compared to normal and recovery which can be attributed to its phosphorylation upon HS. We also detected conversion of lamin Dm1 into Dm2 isoform (disappearance of the faster migrating (lower) band and strengthening of the slower (upper) band upon HS compared to normal and recovery which indicates transient lamin phosphorylation, attributed to HS disappearing upon recovery. Using S25-specific monoclonal antibodies (recognizing unphosphorylated protein) we demonstrated that this conversion is the result of at least one phosphorylation which takes place at S25. We demonstrated that the change in the level of S25 phosphorylation after heat shock is statistically significant in both Kc and S2 cells. We showed previously using *in vitro* nuclear assembly system and transient transfection studies as well as solubility assay that lamin Dm S25 phospho-mimicking (pseudophosphorylation) mutant demonstrated a lower percentage of alpha-helical structure, lower polymerization properties, higher solubility and lower affinity for association with chromatin [3]. This suggests that *in vivo*, upon HS, such modified lamin Dm may be more soluble and may participate in new interactions, possibly also in different locations. Since mammalian lamin A when phosphorylated at the N-terminal domain at the N-terminal Cdk1 (“mitotic”) site relocates to the nuclear interior from the nuclear lamina we may presume that S25 phosphorylation on lamin Dm may result in similar relocation and modified interactions [4]; [5]; [6]. S25 in lamin Dm is not a Cdk1-specific site but epitope mapping studies on lamin Dm point mutants suggested that such modification may affect N-terminal lamin Dm structure up to the beginning of alpha-helical rod domain [3]. For a deeper discussion on the correlation of phosphorylation and lamin properties see [7].

Our IF studies indicated that upon HS a fraction of Top2 relocates from homogenous, intranuclear distribution into lateral, sub-lamina distribution with frequently seen, spherical Top2-dense granules, and the relocation is reversible. It was demonstrated previously that Top2 can exist in different fractions differing in interactions. [46], [49], solubility, phosphorylation and activity [8]. Therefore we may suggest that the demonstrated relocation indicated that a fraction of Top2 may interact with different protein complexes at the nuclear lamina with lamin Dm as well. This hypothesis has been supported by lamins and Top2 proteome analyses (unpublished data, manuscript in preparation - see PhD thesis of Marta Rowinska [72]). Other fractions present in “granules” may represent interactions with stress granules protein complexes forming at the cell nucleus. Indeed our Top2 proteome data confirm the Top2 complexes with stress granule proteins (Marta Rowinska PhD thesis, manuscript in preparation. Previously reported Top2 fraction associated with RNA particles.may fit into both populations [73]. Top2 relocation upon HS was confirmed also on embryos

which suggests that this is a common mechanism for Top2 relocation in response to HS. It should be pointed out that detected relocations of proteins are fully reversible upon recovery. Although we did not quantify any obvious relocation of lamin Dm, a weaker signal in nuclear envelope showed by IF together with stable protein level showed by WB suggest that some lamin dispersion and relocation to nucleoplasm is possible, but it remains below the sensitivity our detection methods. The other possible explanation is participation in new multiprotein complexes containing RNA and DNA both at the NL and internally, which might limit accessibility of antibodies to lamin Dm. Please note that we have not detected any changes in lamin C mobility neither location. Detection of statistically significant relocation of chromatin in third instar larvae polyploid nuclei to the nuclei periphery and/or sub-lamina location together with lamin Dm disappearance from the nucleus interior and migration to the nuclear lamina, together with detected Top2 relocation to the nuclear lamina strongly suggest that the significant remodelling of chromatin interactions and Top2 and lamin Dm interactions, as well as binding partners, may occur. This suggests also the potential involvement in the reorganization of chromatin, potential general gene expression modification, which we know takes place upon HS, and modified lamin Dm and Top2 interactions with nucleic acids.

Solubility studies analyzing an amount of particular protein presence in a particular fraction upon sequential extraction confirmed our hypothesis that HS affect relocation and/or posttranslational modification which is also correlated with modified solubility which in turn suggests modified properties and/or interactions, or both. We used three steps of extractions with such concentration of salt to reflect the most frequent conditions used for extraction of specific fractions of nuclear proteins. The lower salt concentration allows maintenance of “soluble proteins” in isolated or lyzed cell nuclei while 150 mM salt extracts the majority of “soluble” proteins. Half molar salt has been typically used for extraction of a major fraction of lamins both in mammalian and fly model systems of tissue cultured cells [9]. Since we detected statistically significant changes in the amount of most tested proteins in many fractions upon HS, with the highest frequency in 150 mM fraction, we may suggest that HS induces significant changes in properties and/or interactions of many proteins. This also nicely fit into previous studies’ results that different fractions of lamin Dm and Top2 were discovered in fly cells with different properties, phosphorylation, chromatin interaction and activity. Similar data were obtained on embryos. In S2 cells changes in Top2 “solubility” are not statistically significant so this might be the result of a different set of proteins present in Kc and S2 cells (as they derive from different developmental stages).

Immunoprecipitation studies demonstrated co-precipitation of lamin Dm with Top2 and Top2 with lamin Dm under native and “denaturing” (crosslinking) conditions. Surprisingly some of the lamin Dm -Top2 interactions were nucleic acid-dependent which suggests that both proteins may interact or localize as neighbors on nucleic acid/DNA next to each other. Alternatively, they may interact indirectly with protein partners of complexes residing on DNA/RNA. Please remember that both proteins interact *in vivo* with DNA and RNA [50]; [49] while Top2 was found in complexes with

RNA in fly cells [73]. Although only a fraction of lamin Dm and Top2 interact and colocalize with each other, HS induction significantly changes the colocalization between them in Kc cells and larvae cells as indicated by PLA studies. Also, co-precipitation studies suggest that heat shock increased interaction. Interestingly lamin Dm isoforms co-precipitated with Top2 reflecting the same pattern as the entire population of lamin Dm under HS. Note the presence of predominant Dm2 isoform and barely detected Dm1 form after IP. This indicates that the phosphorylation state at S25 does not significantly affect lamin Dm binding to Top2 and *vice versa* which might suggest that lamin head domain and very first part of rod domain does not participate in interactions with Top2. Presented data suggest an increase of binding induced by HS. Detected increased binding of lamin Dm and Top2 to chromatin *in vivo* and a several-fold increase of binding by Top2 may be in agreement with previous studies (80-90-ties) on new HS-induced *in vivo* binding sites. The detection of both DNA and RNA bound is also in agreement with previous discoveries [1]. Also interesting seems to be results from fractionation for *in vivo* crosslinking and chromatin binding studies. Identification of the “soluble” fraction of lamin Dm and Top2 as the most efficient in binding to nucleic acid confirms different properties of different fractions of both proteins in chromatin association and “karyoskeletal” function. Since we detected relocation of the proteins upon HS and it has been confirmed that HS resulted in the relocation of lamin Dm and Top2 into an “insoluble” fraction we suggest this fraction has a different interactome and may predominantly localize to nuclear lamina where the chromatin interactions with presumably heterochromatin (constitutive and/or HS induced) are maintained by other protein complexes while Top2 still retains or, as PLA studies indicated increases its presence. The full recovery of “normal” Top2 and lamin Dm interactions upon recovery confirms that this is a reversible, fully physiological process by which cells evolved to survive and resist potential risk of damage to the cells upon HS conditions. In order to interconnect lamin Dm and Top2 role upon stress induction with changes in their proteomes, gene expression regulation and chromatin sites binding we analysed changes in lamins and Top2 proteome together with RNAseq and ChIPseq data (manuscripts in preparation). Preliminary data already obtained suggest a nice correlation with the data presented in this work.

COMPETING INTERESTS

The authors declare that they have no competing interests.

REFERENCES

[1] G. I. Evan and D. C. Hancock, “Studies on the interaction of the human c-myc protein with cell nuclei: p62c-myc as a member of a discrete subset of nuclear proteins.,” *Cell*, vol. 43, no. 1, pp. 253–61, 1985.

[2] P. A. Fisher, M. McConnell, A. Greenleaf, J. Lee, and D. E. Smith, “Heat shock-induced appearance of RNA polymerase II in karyoskeletal protein-enriched (nuclear ‘matrix’) fractions correlates with transcriptional shutdown in Drosophila melanogaster.,” *J. Biol. Chem.*, vol. 264, no. 6, pp. 3464–9, 1989.

[3] M. McConnell, A. M. Whalen, D. E. Smith, and P. A. Fisher, “Heat shock-induced changes in the structural stability of proteinaceous karyoskeletal elements in vitro and morphological effects in situ.,” *J. Cell Biol.*, vol. 105, no. 3, pp. 1087–98, 1987.

[4] W. C. Earnshaw and Heck, “Localization of topoisomerase II in mitotic chromosomes.,” *J. Cell Biol.*, vol. 100, no. 5, pp. 1716–25, 1985.

[5] S. M. Gasser, J. F. Laroche, E. B. d. l. Tour, and U. K. Laemmli, “Metaphase chromosome structure. Involvement of topoisomerase II,” *J. Mol. Biol.*, vol. 188, no. 4, pp. 613–29, 1986.

[6] W. C. Earnshaw, B. Halligan, C. A. Cooke, M. M. Heck, and L. F. Liu, “Topoisomerase II is a structural component of mitotic chromosome scaffolds.,” *J. Cell Biol.*, vol. 100, no. 5, pp. 1706–15, 1985.

[7] R. Rzepecki, E. Markiewicz, and J. Szopa, “Identification of the proteins responsible for SAR DNA binding in nuclear matrix of Cucurbita pepo.,” *Acta Biochim. Pol.*, vol. 42, no. 2, pp. 171–176, 1995.

[8] R. Rzepecki, E. Markiewicz, R. Adamiec, and J. Szopa, “Interaction of the Pisum sativum nuclear matrix proteins with SAR DNA.,” *Acta Biochim. Pol.*, vol. 42, no. 1, pp. 75–81, 1995.

[9] T. Dechat, S. A. Adam, P. Taimen, T. Shimi, and R. D. Goldman, “Nuclear lamins.,” *Cold Spring Harb. Perspect. Biol.*, vol. 2, no. 11, pp. 1–22, 2010.

[10] X. Wong, A. J. Melendez-Perez, and K. L. Reddy, “The Nuclear Lamina.,” *Cold Spring Harb. Perspect. Biol.*, vol. 14, no. 2, Feb. 2022.

[11] S. Osmanagic-Myers, T. Dechat, and R. Foisner, “Lamins at the crossroads of mechanosignaling,” *Genes Dev.*, vol. 29, no. 3, pp. 225–237, 2015.

[12] S. R. Iyer, E. S. Folker, and R. M. Lovering, “The Nucleoskeleton: Crossroad of Mechanotransduction in Skeletal Muscle,” *Front. Physiol.*, vol. 12, no. October, pp. 1–8, 2021.

[13] F. Donnaloja, F. Carnevali, E. Jacchetti, and M. T. Raimondi, “Lamin A/C Mechanotransduction in Laminopathies,” *Cells*, vol. 9, no. 5, 2020.

[14] K. L. Wilson and R. Foisner, “Lamin-binding Proteins,” pp. 1–17, 2010.

[15] M. Dubinska-Magiera, M. Zaremba-Czogalla, and R. Rzepecki, “Muscle development, regeneration and laminopathies: How lamins or lamina-associated proteins can contribute to muscle development, regeneration and disease,” *Cell. Mol. Life Sci.*, vol. 70, no. 15, pp. 2713–2741, 2013.

[16] R. Rzepecki and P. A. Fisher, “In vivo phosphorylation of Drosophila melanogaster nuclear lamins during both interphase and mitosis,” *Cell. Mol. Biol. Lett.*, vol. 7, no. 3, pp. 859–876, 2002.

[17] M. Zaremba-Czogalla, K. Piekarowicz, K. Wachowicz, K. Kozioł, M. Dubińska-Magiera,

and R. Rzepecki, “The different function of single phosphorylation sites of Drosophila melanogaster lamin Dm and lamin C,” *PLoS One*, vol. 7, no. 2, 2012.
[18] M. Machowska, K. Piekarowicz, and R. Rzepecki, “Regulation of lamin properties and functions: Does phosphorylation do it all?,” *Open Biol.*, vol. 5, no. 11, 2015.
[19] F. Napoletano *et al.*, “The prolyl-isomerase PIN1 is essential for nuclear Lamin-B structure and function and protects heterochromatin under mechanical stress.,” *Cell Rep.*, vol. 36, no. 11, p. 109694, Sep. 2021.
[20] M. Pałka *et al.*, “Laminopathies: what can humans learn from fruit flies,” *Cell. Mol. Biol. Lett.*, vol. 23, no. 1, pp. 1–12, 2018.
[21] R. Rzepecki and Y. Gruenbaum, “Invertebrate models of lamin diseases,” *Nucleus*, vol. 9, no. 1, pp. 227–234, 2018.
[22] M. Zaremba-Czogalla *et al.*, “Identification of new in vivo phosphosites on lamin Dm-the evidence of heterogeneity of phosphorylation sites in different Drosophila tissues,” *Nucleus*, vol. 2, no. 5, 2011.
[23] U. Schneider, T. Mini, P. Jenö, P. A. Fisher, and N. Stuurman, “Phosphorylation of the major Drosophila lamin in vivo: Site identification during both M-phase (Meiosis) and interphase by electrospray ionization tandem mass spectrometry,” *Biochemistry*, vol. 38, no. 14, pp. 4620–4632, 1999.
[24] N. Stuurman, N. Maus, and P. A. Fisher, “Interphase phosphorylation of the Drosophila nuclear lamin: Site-mapping using a monoclonal antibody,” *J. Cell Sci.*, vol. 108, no. 9, pp. 3137–3144, 1995.
[25] J. M. Berger and J. C. Wang, “Recent developments in DNA topoisomerase II structure and mechanism,” *Curr. Opin. Stuctural Biol.*, vol. 6, no. 1, pp. 84–90, 1996.
[26] J. Roca and J. . Wang, “DNA transport by a type II DNA topoisomerase: evidence in favor of a two-gate mechanism.,” *Cell*, vol. 77, no. 4, pp. 609–16, 1994.
[27] J. Roca, J. M. Berger, S. C. Harrison, and J. C. Wang, “DNA transport by a type II topoisomerase: direct evidence for a two-gate mechanism,” *Proc. Natl. Acad. Sci. U. S. A.*, vol. 93, no. 9, pp. 4057–62, 1996.
[28] J. Roca, “Topoisomerase II: a fitted mechanism for the chromatin landscape.,” *Nucleic Acids Res.*, vol. 37, no. 3, pp. 721–730, Feb. 2009.
[29] E. M. Hildebrand *et al.*, “Mitotic chromosomes are self-entangled and disentangle through a topoisomerase-II-dependent two-stage exit from mitosis.,” *Mol. Cell*, vol. 84, no. 8, pp. 1422-1441.e14, Apr. 2024.
[30] P. Buchenau, H. Saumweber, and D. J. Arndt-Jovin, “Consequences of topoisomerase II inhibition in early embryogenesis of Drosophila revealed by in vivo confocal laser scanning microscopy.,” *J. Cell Sci.*, vol. 104 (Pt 4, pp. 1175–85, 1993.
[31] S. DiNardo, R. Voelkel, and R. Sternglanz, “DNA topoisomerase II mutant of Saccharomyces cerevisiae: topoisomerase II is required for segregation of daughter molecules at the termination of DNA replication,” *Proc. Natl. Acad. Sci. U. S. A.*, vol. 81, no. 9, pp. 2616–20, 1984.
[32] C. Holm, T. Goto, J. C. Wang, and D. Botstein, “DNA topoisomerase II is required at the time of mitosis in yeast.,” *Cell*, vol. 41, no. 2, pp. 553–63, 1985.
[33] M. Iwai, A. Hara, T. Andoh, and R. Ishida, “ICRF-193, a catalytic inhibitor of DNA topoisomerase II, delays the cell cycle progression from metaphase, but not from anaphase to the G1 phase in mammalian cells,” *FEBS Lett.*, vol. 406, no. 3, pp. 267–70, 1997.
[34] J. B. Rattner, M. J. Hendzel, C. S. Furbee, M. T. Muller, and D. P. Bazett-Jones,

"Topoisomerase II alpha is associated with the mammalian centromere in a cell cycle- and species-specific manner and is required for proper centromere/kinetochore structure," *J. Cell Biol.*, vol. 134, no. 5, pp. 1097–107, 1996.

[35] C. E. Shamu and A. W. Murray, "Sister chromatid separation in frog egg extracts requires DNA topoisomerase II activity during anaphase.," *J. Cell Biol.*, vol. 117, no. 5, pp. 921–34, 1992.

[36] T. Uemura, H. Ohkura, Y. Adachi, K. Morino, K. Shiozaki, and M. Yanagida, "DNA topoisomerase II is required for condensation and separation of mitotic chromosomes in S. pombe," *Cell*, vol. 50, no. 6, pp. 917–25, 1987.

[37] Y. Adachi, M. Luke, and U. K. Laemmli, "Chromosome assembly in vitro: topoisomerase II is required for condensation.," *Cell*, vol. 64, no. 1, pp. 137–48, 1991.

[38] W. I. Garinther and M. C. Schultz, "Topoisomerase function during replication-independent chromatin assembly in yeast.," *Mol. Cell. Biol.*, vol. 17, no. 7, pp. 3520–3526, Jul. 1997.

[39] E. R. Wood and W. C. Earnshaw, "Mitotic chromatin condensation in vitro using somatic cell extracts and nuclei with variable levels of endogenous topoisomerase II.," *J. Cell Biol.*, vol. 111, no. 6 Pt 2, pp. 2839–2850, Dec. 1990.

[40] F. Klein, T. Laroche, M. E. Cardenas, J. F. Hofmann, D. Schweizer, and S. M. Gasser, "Localization of RAP1 and topoisomerase II in nuclei and meiotic chromosomes of yeast.," *J. Cell Biol.*, vol. 117, no. 5, pp. 935–948, Jun. 1992.

[41] P. B. Moens and W. C. Earnshaw, "Anti-topoisomerase II recognizes meiotic chromosome cores.," *Chromosoma*, vol. 98, no. 5, pp. 317–322, Nov. 1989.

[42] D. Rose, W. Thomas, and C. Holm, "Segregation of recombined chromosomes in meiosis I requires DNA topoisomerase II.," *Cell*, vol. 60, no. 6, pp. 1009–1017, Mar. 1990.

[43] D. Rose and C. Holm, "Meiosis-specific arrest revealed in DNA topoisomerase II mutants.," *Mol. Cell. Biol.*, vol. 13, no. 6, pp. 3445–3455, Jun. 1993.

[44] M. Berrios, N. Osheroff, and P. A. Fisher, "In situ localization of DNA topoisomerase II, a major polypeptide component of the Drosophila nuclear matrix fraction.," *Proc. Natl. Acad. Sci. U. S. A.*, vol. 82, no. 12, pp. 4142–4146, Jun. 1985.

[45] P. A. Fisher, "Chromosomes and chromatin structure: the extrachromosomal karyoskeleton.," *Curr. Opin. Cell Biol.*, vol. 1, no. 3, pp. 447–453, Jun. 1989.

[46] V. H. Meller, P. A. Fisher, and M. Berrios, "Intranuclear distribution of DNA topoisomerase II and chromatin.," *Chromosom. Res. an Int. J. Mol. Supramol. Evol. Asp. Chromosom. Biol.*, vol. 3, no. 4, pp. 255–260, Jun. 1995.

[47] A. M. Whalen, M. McConnell, and P. A. Fisher, "Developmental regulation of Drosophila DNA topoisomerase II.," *J. Cell Biol.*, vol. 112, no. 2, pp. 203–213, Jan. 1991.

[48] F. Girard, B. Bello, U. K. Laemmli, and W. J. Gehring, "In vivo analysis of scaffold-associated regions in Drosophila: A synthetic high-affinity SAR binding protein suppresses position effect variegation," *EMBO J.*, vol. 17, no. 7, pp. 2079–2085, 1998.

[49] R. Rzepecki and P. a Fisher, "During both interphase and mitosis, DNA topoisomerase II interacts with DNA as well as RNA through the protein's C-terminal domain.," *J. Cell Sci.*, vol. 113, pp. 1635–1647, 2000.

[50] R. Rzepecki, S. S. Bogachev, E. Kokoza, N. Stuurman, and P. A. Fisher, "In vivo association of lamins with nucleic acids in Drosophila melanogaster," vol. 129, pp. 121–129, 1998.

[51] N. Wagner, D. Weber, S. Seitz, and G. Krohne, "The lamin B receptor of Drosophila melanogaster," *J. Cell Sci.*, vol. 117, no. 10, pp. 2015–2028, 2004.

[52] U. K. Laemmli, “Cleavage of structural proteins during the assembly of the head of bacteriophage T4.,” *Nature*, vol. 227, no. 5259, pp. 680–685, Aug. 1970.
[53] E. Harlow and D. Lane, “Storing and purifying antibodies.,” *Cold Spring Harb. Protoc.*, vol. 1988, pp. 283–318.
[54] R. Rzepecki and P. A. Fisher, “The study of Drosophila melanogaster lamin Dm phosphorylation in tissue culture Kc cells in vivo,” *Cell. Mol. Biol. Lett.*, vol. 05, no. 2, p. 263, 2000.
[55] D. E. Smith, Y. Gruenbaum, M. Berrios, and P. A. Fisher, “Biosynthesis and Interconversion of Drosophila Nuclear Lamin Isoforms during Normal Growth and in Response to Heat Shock,” *J. Cell Biol.*, vol. 105, no. 2, pp. 771–790, 1987.
[56] D. Riemer, N. Stuurman, M. Berrios, C. Hunter, P. A. Fisher, and K. Weber, “Expression of Drosophila lamin C is developmentally regulated: analogies with vertebrate A-type lamins.,” *J. Cell Sci.*, vol. 108 (Pt 1, pp. 3189–3198, 1995.
[57] L. R. Alagar Boopathy, S. Jacob-Tomas, C. Alecki, and M. Vera, “Mechanisms tailoring the expression of heat shock proteins to proteostasis challenges,” *J. Biol. Chem.*, vol. 298, no. 5, p. 101796, 2022.
[58] S. S. Teves and S. Henikoff, “The heat shock response: A case study of chromatin dynamics in gene regulation,” *Biochem. Cell Biol.*, vol. 91, no. 1, pp. 42–48, 2013.
[59] M. Fritsch and C. Wu, “Phosphorylation of Drosophila heat shock transcription factor,” *Cell Stress and Chaperones*, vol. 4, no. 2. pp. 102–117, 1999.
[60] A. Udvardy and P. Schedl, “The dynamics of chromatin condensation: redistribution of topoisomerase II in the 87A7 heat shock locus during induction and recovery,” *Mol. Cell. Biol.*, vol. 13, no. 12, pp. 7522–7530, 1993.
[61] T. C. Rowe, J. C. Wang, and L. F. Liu, “In vivo localization of DNA topoisomerase II cleavage sites on Drosophila heat shock chromatin,” *Mol. Cell. Biol.*, vol. 6, no. 4, pp. 985–992, 1986.
[62] P. Majumder and D. Dasgupta, “Effect of DNA groove binder distamycin a upon chromatin structure,” *PLoS One*, vol. 6, no. 10, 2011.
[63] M. L. Kopka, C. Yoon, D. Goodsell, P. Pjura, and R. E. Dickerson, “The molecular origin of DNA-drug specificity in netropsin and distamycin,” *Proc. Natl. Acad. Sci. U. S. A.*, vol. 82, no. 5, pp. 1376–1380, 1985.
[64] M. E. Ludérus *et al.*, “Binding of matrix attachment regions to lamin B1.,” *Cell*, vol. 70, no. 6, pp. 949–959, Sep. 1992.
[65] E. Kas, L. Poljak, Y. Adachi, and U. K. Laemmli, “A model for chromatin opening: Stimulation of topoisomerase II and restriction enzyme cleavage of chromatin by distamycin,” *EMBO J.*, vol. 12, no. 1, pp. 115–126, 1993.
[66] S. M. Gasser and U. K. Laemmli, “Improved methods for the isolation of individual and clustered mitotic chromosomes,” *Exp. Cell Res.*, vol. 173, no. 1, pp. 85–98, 1987.
[67] D. E. Smith, Y. Gruenbaum, M. Berrios, and P. A. Fisher, “Biosynthesis and interconversion of Drosophila nuclear lamin isoforms during normal growth and in response to heat shock,” *J. Cell Biol.*, vol. 105, no. 2, pp. 771–790, 1987.
[68] D. E. Smith and P. A. Fisher, “Identification, developmental regulation, and response to heat shock of two antigenically related forms of a major nuclear envelope protein in Drosophila embryos: application of an improved method for affinity purification of antibodies using polypeptide,” *J. Cell Biol.*, vol. 99, no. 1 Pt 1, pp. 20–28, Jul. 1984.
[69] V. Kochin *et al.*, “Interphase phosphorylation of lamin A,” *J. Cell Sci.*, vol. 127, no. 12, pp. 2683–2696, 2014.

[70] N. Naetar *et al.*, “LAP2alpha maintains a mobile and low assembly state of A-type lamins in the nuclear interior.,” *Elife*, vol. 10, Feb. 2021.
[71] J.-T. Chen *et al.*, “Identification of the lamin A/C phosphoepitope recognized by the antibody P-STM in mitotic HeLa S3 cells.,” *BMC Biochem.*, vol. 14, p. 18, Jul. 2013.
[72] M. Rowińska, “Identification of protein artners of lamin Dm and topoisomerase II under heat shock conditions in Drosophila melanogaster model system,” 2024. [Online]. Available: https://bip.uni.wroc.pl/3543/postepowanie-w-sprawie-nadania-stopnia-doktora-w-dziedzinie-nauk-scislych-i-przyrodniczych-w-dyscyplinie-nauki-biologiczne-mgr-marta-rowinska.html.
[73] V. H. Meller and P. A. Fisher, “Nuclear distribution of Drosophila DNA topoisomerase II is sensitive to both RNase and DNase.,” *J. Cell Sci.*, vol. 108 (Pt 4, pp. 1651–1657, Apr. 1995.
[74] V. Pekovic *et al.*, “Nucleoplasmic LAP2alpha-lamin A complexes are required to maintain a proliferative state in human fibroblasts.,” *J. Cell Biol.*, vol. 176, no. 2, pp. 163–172, Jan. 2007.

FIGURE LEGENDS

Figure 1

The expression of heat-inducible Hsp70 protein is an excellent indicator of the efficiency of stress and recovery

To examined the effect of recovery western blot analysis was performed (A) similarly on both cell lines. Besides Hsp70, Hsf was used as a stress indicator, α- tubulin (α-Tub) was used as a loading control. Protein levels were verified at various time points after 1h HS and recovery after 6/24/48/72/96h (right away after HS), N conditions were used as a reference for complete R. Additionally, the relative expression (B) of selected transcripts (*Hsf, Hsp22, Hsp68, Hsp70, Hsp83; Tub84b* was used as a reference gene) in Kc cells was examined by RT-qPCR during different HS time points (15-, 30- and 60-minutes).

The efficiency of heat shock induction and recovery was confirmed by immunofluorescence staining of Kc (C) and S2 (D) cells in different conditions: N - normal, HS - heat shock (1h) and R - recovery. Panels A and B show, chromatin (DAPI - blue), topoisomerase II (Top2 - green), heat shock induction indicated by heat shock protein (Hsp70 - red) and lamin Dm (Lam Dm - grey), and merge. Scale bars = 5 μm. Magnification 63x.

Figure 2

The effect of stress on gene and protein expression

Panels A and B show relative expression for specific genes of interest in Kc and S2 cells. Bars represent the fold change of the transcript level after 1h heat shock induction for Kc (black) and S2 (grey). The error bars represent the standard deviation from the mean of fold change, of 3 biological replicates, calculated by Applied Biosystems™ qPCR analysis module, connected with QuantStudio™ 5 thermocycler. For the final results calculations, the ΔΔCt method with the normalization on control cells (N) and the set of endogenous controls (18S/28S/Tub84B/Act5C) was used. Panel A shows genes of interest: Lam Dm, Lam C*, Top2, and Hsf for both cell types. A bar graph on panel B shows the relative expression of Hsp representatives (Hsp83, Hsp22, Hsp68, Hsp70).

Total protein level (Top2, Lam Dm, Hsf, HDAC1, Hsp70, α-Tub) and non-phosphorylated Lam Dm - designated as ADL84 (referring to the antibodies used) in N, HS and R (72h in Kc and 48h in S2 cells) condition was examined on Kc (C) and S2 cells (D). The statistical analysis from densitometry signal only for significant changes after HS (presented on the right from WB panels on C and D panels). The last lane marked as N48h/72h represents data from secondary control - cells cultivated the same duration of time as cells during recovery – R but without HS induction. For the statistical analysis of densitometric measurements, α-Tubulin was used as a normalization factor.

*Please note that Lam C transcripts were also detected in S2 cells (about 31st cycle), ~ 7 qPCR cycles after detection in Kc cells. In S2 cells the protein was undetectable.

Figure 3
Stress affects the phosphorylation of lamin Dm S25

Changes in the patterns of lamin Dm phosphorylation between N and HS conditions were examined by immunofluorescence staining of Kc cells (A). Visualization of unphosphorylated Lam Dm on S25 (using ADL84 antibodies) reveals decreased IF signal after HS. Panels showing chromatin (DAPI - blue), lamin Dm (Lam Dm - green), dephosphorylation of lamin Dm on S25 (red) and merge visualization. Scale bars = 5 µm. Magnification 63x.

The effect was confirmed by western blot analysis of total lamin Dm and unphosphorylated S25 variant performed on Kc (B) and S2 (C) cell lines. Staining with ADL84 antibodies shows the reversible decrease of lamin unphosphorylated on S25 after 1h HS, while a total pool of lamin Dm (both Dm1 and Dm2) is stable in response to HS. Relative band intensity quantification of total and unphosphorylated Lam Dm based on densitometric analysis of western blots was also performed (lower graphs on panels B and C). The presented data based on of 3 biological replicates (each at least 2 technical replicates). The statistical analysis was performed (t-student test) to indicate the differences in phosphorylation status after heat shock induction. Comparison of N to HS showed the decrease of signal from unphosporylates Lam Dm S25 (B - Kc cells: $p \leq 0{,}0001$ and C – S2 cells: $p < 0{,}015$) while maintaining the same signal intensity from total Lam Dm. For the statistical analysis of densitometric measurements, α-tubulin was used as a normalization factor.

Figure 4
Stress reversibly relocalizes Top2

Immunofluorescence staining of Kc cells (A and C) and *D. melanogaster* embryos (B) shows stress-induced Top2 which is reversible upon recovery. Distribution of Top2, Lam Dm (A and B), and LamC (C and D) was analyzed in N, HS and R conditions. IF panels A-D (depending on the staining variant) show chromatin (DAPI - blue), Top2 (green), lamin Dm (Lam Dm – grey/ red), lamin C (grey/red), heat shock induction (Hsp70 - red) and merge visualization. Scale bars = 5 µm. Additionally, panels B and D show fluorescence intensity analysis along white lines visible on merge visualisations. Top2 rearrangement (E) and chromatin rearrangement (G) after heat shock were presented in the graphs as normalized values (the number of counted cell nuclei marked on the graphs as n). Top2 rearrangement (E) statistics (chi-squared test; $p=1{,}9*10E-27$) was calculated based on the cell nuclei counted in *D. melanogaster* embryonic cells; chromatin rearrangement (G) was calculated based on cell nuclei counted in 3rd instar larvae cells (chi-squared test; $p=6{,}62*10E-8$). Representative staining is shown on the F graph for Top2 rearrangement and on H for chromatin rearrangement.

Figure 5

Stress affects the solubility of lamin Dm and other nuclear proteins in Kc and S2 cells

A solubility assay verified by western blot analysis showed differences between the solubility levels of proteins (Lam, Top2, HDAC1, Hsf, Hsp70) under N and HS (1h) conditions in Kc (A) and S2 cells (B). Data on bar graphs (C – Kc cells and D – S2 cells) were plotted as the percentage of output lysate which was considered as 100% for each replicate. The statistics (t-student test) on the bar graphs show the comparison of N versus HS conditions for each fraction independently. Above each plot, the number of repetitions (n) taken for the statistical analysis is given. White bars in each graph refer to normal conditions (N - 23°C), grey to heat shock induction (HS – 1h, 37°C). Subsequent fractions are marked as lysate (control), 50 mM, 150 mM and 500 mM respectively. No significant difference is pointed as "ns",* means p-value<0,05, ** p-value< 0,01, *** p-value<0,001, and **** p<0,0001.

Figure 6

Lamin Dm interacts with Topoisomerase II directly through adjacent chromatin DNA regions and interactions are increased during heat shock

Immunofluorescence staining of cell nuclei from D. melanogaster larvae (A, B – bottom panel), C and J. Chromatin was visualized by DAPI staining (blue), Top2 (green), Lam Dm/ LamC (red). Two left and upper right panels on graph 6A show staining of polytene nuclei (all channels were merged) for Lamin Dm (ADL677; ADL84.12 – phospho- specific), Lamin C (LC28) and Top2 (Rabbit AP IgG). Diploid nuclei (6A lower right panel) are shown separately for staining of Top2 (green) and Lamin Dm (red) and merged. Colocalization was confirmed by PLA assay (B, C, H and J) for Top2 and Lam Dm. Graph B shows colocalization confirmed in the Kc cell line (6B upper) and polytenic nuclei of salivary gland cells from 3rd instar larvae (6B below) with appropriate controls - without antibodies (left) and only with anti-Top2 antibodies (middle). A positive signal was observed only after incubation with both antibodies (Lam Dm and Top2 – right panels). In the supplementary material Figure 6 – video 1 for this figure videos showing the interaction between the tested proteins have been posted presenting polytene chromosomes cell nuclei. Graph C shows a Z-series of those movies. LamDm and Top2 localize in common protein complexes in 3rd instar larvae diploid and polyploid nuclei from proximity ligation assay performed on larval spreads (J). Next, the co-immunoprecipitation analysis anti lamDm and Top2 were performed (D-G). First, the interaction was confirmed with specific rabbit Lam Dm antibodies (used during the IP procedure, while WB staining of lamin Dm was performed with mouse ADL67 antibodies) with the increasing amount of embryo extracts (D).

Direct interaction was confirmed by the WB analysis co-immunoprecipitation performed with affinity-purified anti-lamin Dm (E left) or Top2 (E right) antibodies on native Kc cell extracts. After IP additional S1 micrococcal nuclease treatment was performed a positive signal was observed in the treated and untreated samples

confirming a direct effect. Also, during IP (anti Lam Dm and anti Top2) in cross-linking conditions (1% PFA) in Kc cell line Lam Dm and Top2 co-immunoprecipitated (F) in both N and HS conditions. co-IP as well as WB staining was performed with RαLamDm and RαTop2 specific antibodies (n=3). Zoom to the line of lamin Dm with separated Dm1 and Dm2 lines indicated (G) shows lamin Dm conversion after heat shock induction. The increased signal from the interaction of Lam Dm and Top2 was observed after HS after PLA assay was performed in the Kc cell line (H). Statistical analysis of Kc PLA assay (I) showed statistical significance, quantification of PLA performed on Kc cells, approximately 100 nuclei were counted for each condition, ANOVA test applied, $p<0,01$.

Figure 7

Stress induces the association of lamin Dm and Topoisomerase II with chromatin DNA

Graph A shows a western blot (WB) and autoradiography (^{32}P) analysis of immunoprecipitation performed with affinity-purified anti-lamin Dm antibodies on native Kc cell extracts. After IP additional micrococcal nuclease treatment was performed. Graph B shows WB analysis of immunoprecipitation performed with affinity-purified anti-Lam or anti-Top2 on UV cross-linked Kc cell extracts. After IP additional micrococcal nuclease treatment was performed. In both cases membranes after WB were stained with affinity-purified polyclonal anti-Drosophila lamin Dmo-derivatives antibodies (Lam) and affinity-purified polyclonal anti-Drosophila Top2 antibodies (Top2) confirming interactions regardless of the conditions used in the experiments.

The effects of DNase I and RNase A on labelled nucleic acid associated with both lamin Dm and Top2, in normal cell nuclei (N) as well as after heat shock (HS, 1h) was analyzed on panel C. Nuclease treatments after ^{32}P-labeling are indicated below each lane.

Graph D shows WB and ^{32}P analysis of fractionation of ^{32}P labelled and UV cross-linked Kc cell lysate. Untreated lysate (total), soluble and insoluble fractions are shown. Fractionation of protein-bound nucleic acid, NaCl extract (soluble) versus insoluble (‘matrix’) fraction. WB analysis and ^{32}P-labeling are as indicated. Fractions loaded after ^{32}P-labeling are indicated below each lane.

Graph E shows WB and ^{32}P analysis of insoluble fractions of ^{32}P labelled and UV cross-linked Kc cell lysate in normal (N), heat shock (HS) and recovery (Rec) conditions.

Graph F shows WB and ^{32}P analysis of fractions of ^{32}P labelled and UV cross-linked Kc cell lysate in N and HS conditions with (+) and without (-) distamycin treatment.

Graph G shows WB analysis of Hsp70 level in Kc cells after different treatment conditions (indicated on the panel).

SUPPLEMENTARY DATA

Figure 1 – Figure Supplement 1

Heat shock induction in *D. melanogaster* embryos

The efficiency of heat shock induction and recovery was examined by immunofluorescence staining of *D. melanogaster* embryos in different conditions: Normal, Heat shock (1h) and Recovery. Merge, chromatin (DAPI - blue), lamin Dm (Lam Dm - red), and heat shock induction (Hsp70 - green) visualization.

Figure 2 – Figure Supplement 1

Assessment of the gene stability after heat shock induction on *Drosophila melanogaster* cells (Kc and S2) after 1h of HS.

Gene expression for all tested genes (names given on the x-axis) for Kc and S2 cells (A). Bars representing fold change of the transcript level after 1h heat shock induction for Kc (black) and S2 (grey). Only normalization on control (N) was used without further normalization on housekeeping genes. The threshold marked by a dotted line was set as 2 fold. Determination of the most stable reference (housekeeping) genes from a set of tested candidate reference genes was performed using the geNorm algorithm (B). Average expression stability was measured to choose the common endogenous control for Kc and S2 cell lines upon heat shock.

Figure 2 – Figure Supplement 2

List of the primers used for RT-qPCR analysis

Table with a list of all primers used in RT-qPCR analyses. Their sequences, efficiency and source.

Figure 4 – Figure Supplement 1

Analysis of distribution of other nuclear proteins in Kc cells.

Immunofluorescence staining of Kc cells in N, HS (1h) and R condition. Distribution of Hp1 (A – red), Hsf (B - green), HDAC1 (C - green), LBR (D - green) and Pol2Ps5 (E - green). On each graph, chromatin was stained using DAPI (blue). Additionally, Top2 (A - green), Hsp90 (B – red), Lam Dm (C, D and E - red) and bocksbeutel (E- grey) were visualized. . No significant redistribution was observed in the examined conditions. Scale bars = 5 µm.

Figure 4 – Figure Supplement 2

Analysis of distribution of other nuclear proteins in *D. melanogaster* embryos.

Immunofluorescence staining of *D. melanogaster* embryos in N, HS (1h) and R condition with additional fluorescence intensity analysis (A-D). Distribution of Hp1 (A – red), Pol2PS5 (B - green), Hsf (C - green) and HDAC1 (D – green). On each graph, chromatin was stained using DAPI (blue). Additionally Lam Dm (A – green, B-D - red

was visualized. The area from which the fluorescence intensity was analyzed was marked with a yellow line in the “Profile” column on each graph. A graph of the fluorescence intensity distribution (Signal intensity) for each channel is also presented (for each staining separately in the corresponding colour). No significant redistribution was observed in the examined conditions. Scale bars = 5 µm.

Figure 5 – Figure Supplement 1

Solubility assay – a different approach to analysis - validation for the mean intensity of the WB membrane signal

The panels show the same experiment as in Figure 5 with a modified data presentation method. Data was validated for the mean intensity of each band from a given membrane. A solubility assay verified by western blot analysis showed differences between the solubility of proteins (Lam, Top2, HDAC1, Hsf, Hsp70) in N and HS (1h) conditions in Kc (A) and S2 cells (B). White bars in each graph refer to normal conditions (N - 23°C), grey to heat shock induction (HS - 37°C). Subsequent fractions are marked as lysate (control), 50 mM, 150 mM and 500 mM respectively. No significant difference is pointed as “ns”, significant as * p-value<0,05, ** means p-value<0,01, *** p-value<0,001, and **** p<0,0001.

Figure 5 – Figure Supplement 2

Stress affects the solubility of lamin Dm and other nuclear proteins in embryos

The experiment was conducted in the same way as it was performed in the case of Kc and S2 cells. The solubility assay was verified by WB analysis (detected proteins: Hsp70, Lam Dm, Top2, HDAC1 and αTub). The figure shows both approaches to the presentation of the obtained data, which were discussed earlier (B – percentage of lysate and C – validation for mean intensity signal from each membrane). A statistically significant decrease in the lamin Dm solubility after HS in the 50 mM fraction and an increase in Top2 solubility in 150 mM does not reflect the data obtained from the cell culture.

Figure 6 – video 1

PLA movies

The polytenic nuclei of salivary gland cells of the third instar larvae using proximity ligation assay technique (PLA) using anti lamin Dm monoclonal ADL67 antibody and affinity purified anti Top2 antibodies.

Figure 6 – Figure Supplement 1

Cross-linking co-immunoprecipitation performed on S2 cell lines against Lam Dm and Top2

During precipitation in cross-linking conditions of Lam Dm in S2 cells the topoisomerase II co-immunoprecipitated, and conversely. Cells were cross-linked with

1% PFA and then co-immunoprecipitated with antibodies against Lam Dm (A) or Top2 (B). Detection of interaction was performed by immunoblotting with the same antibodies. As a negative control, the same procedure was performed with isotypic antibodies (IgG). No statistical analysis has been carried out.

Figure 1

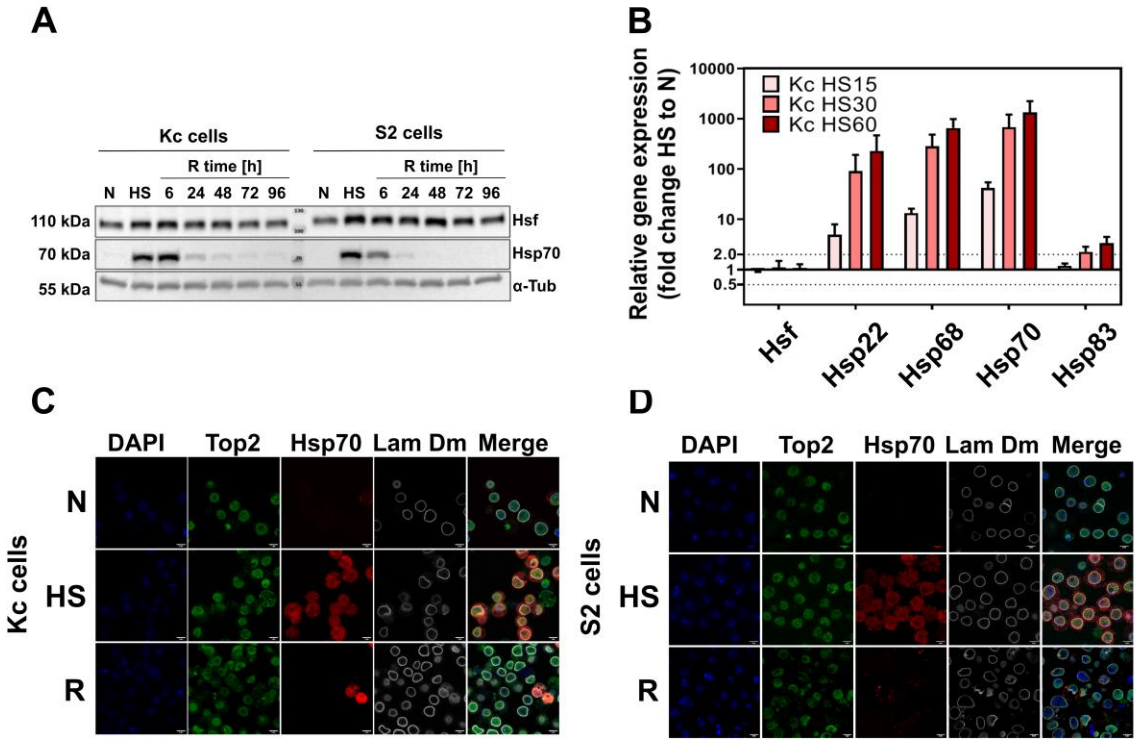

Figure 2

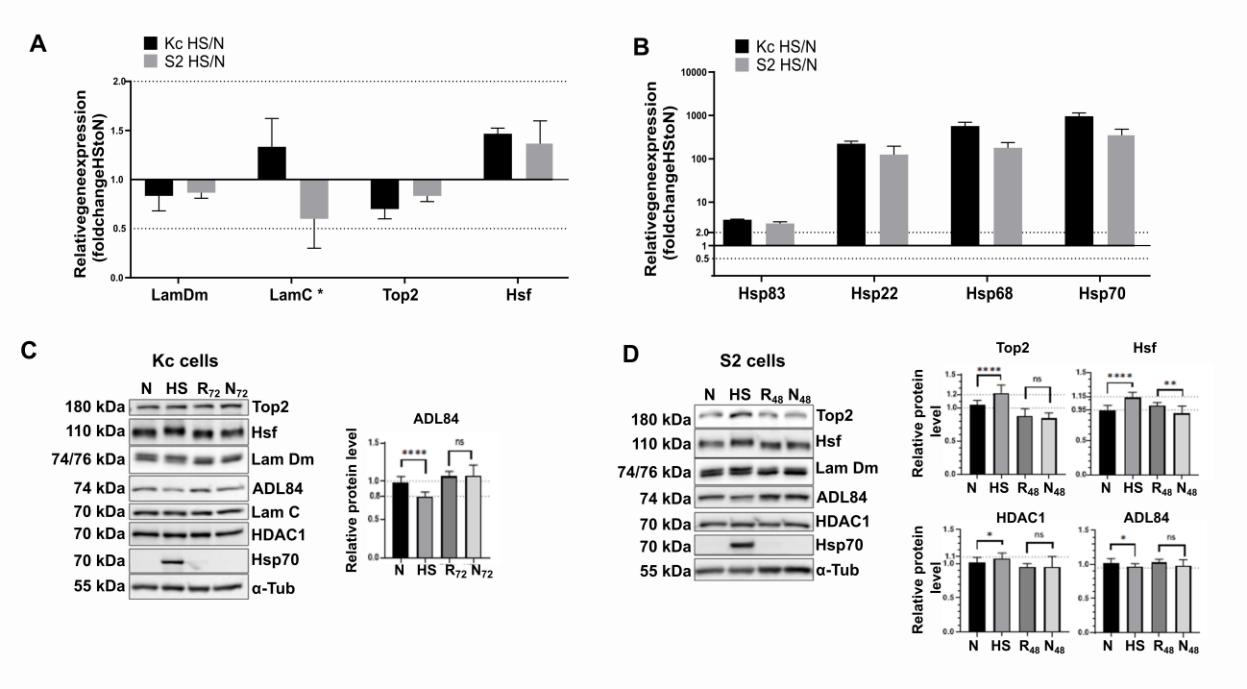

Figure 3

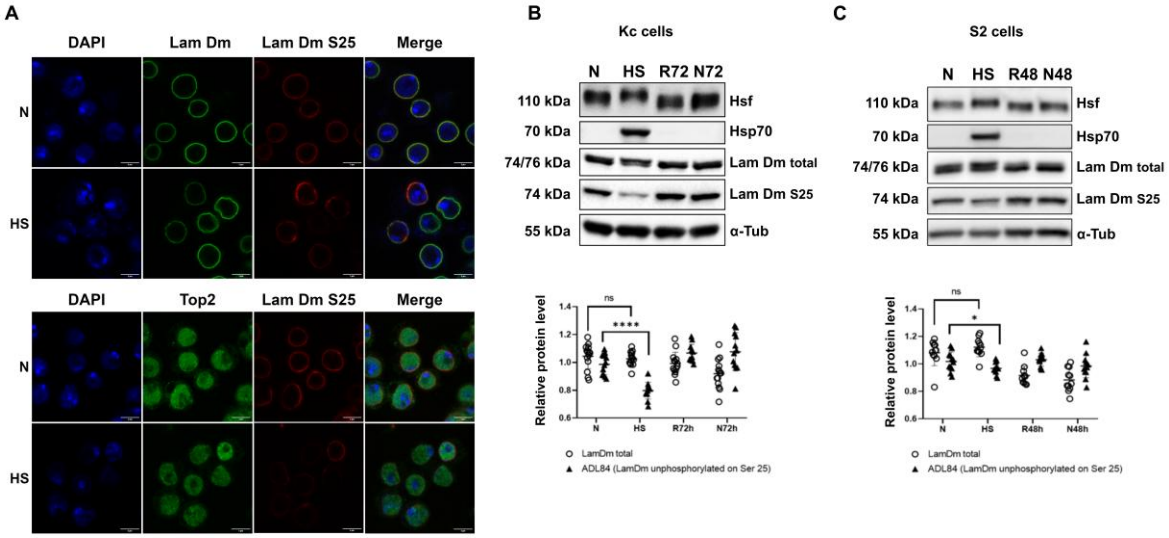
A
DAPI
Lam Dm
Lam Dm S25
Merge
N
HS
DAPI
Top2
Lam Dm S25
Merge
N
HS
B
Kc cells
N HS R72 N72
110 kDa
Hsf
70 kDa
Hsp70
74/76 kDa
Lam Dm total
74 kDa
Lam Dm S25
55 kDa
α-Tub
Relative protein level
ns
****
N
HS
R72h
N72h
LamDm total
ADL84 (LamDm unphosphorylated on Ser 25)
C
S2 cells
N HS R48 N48
110 kDa
Hsf
70 kDa
Hsp70
74/76 kDa
Lam Dm total
74 kDa
Lam Dm S25
55 kDa
α-Tub
Relative protein level
ns
*
N
HS
R48h
N48h
LamDm total
ADL84 (LamDm unphosphorylated on Ser 25)

Figure 4

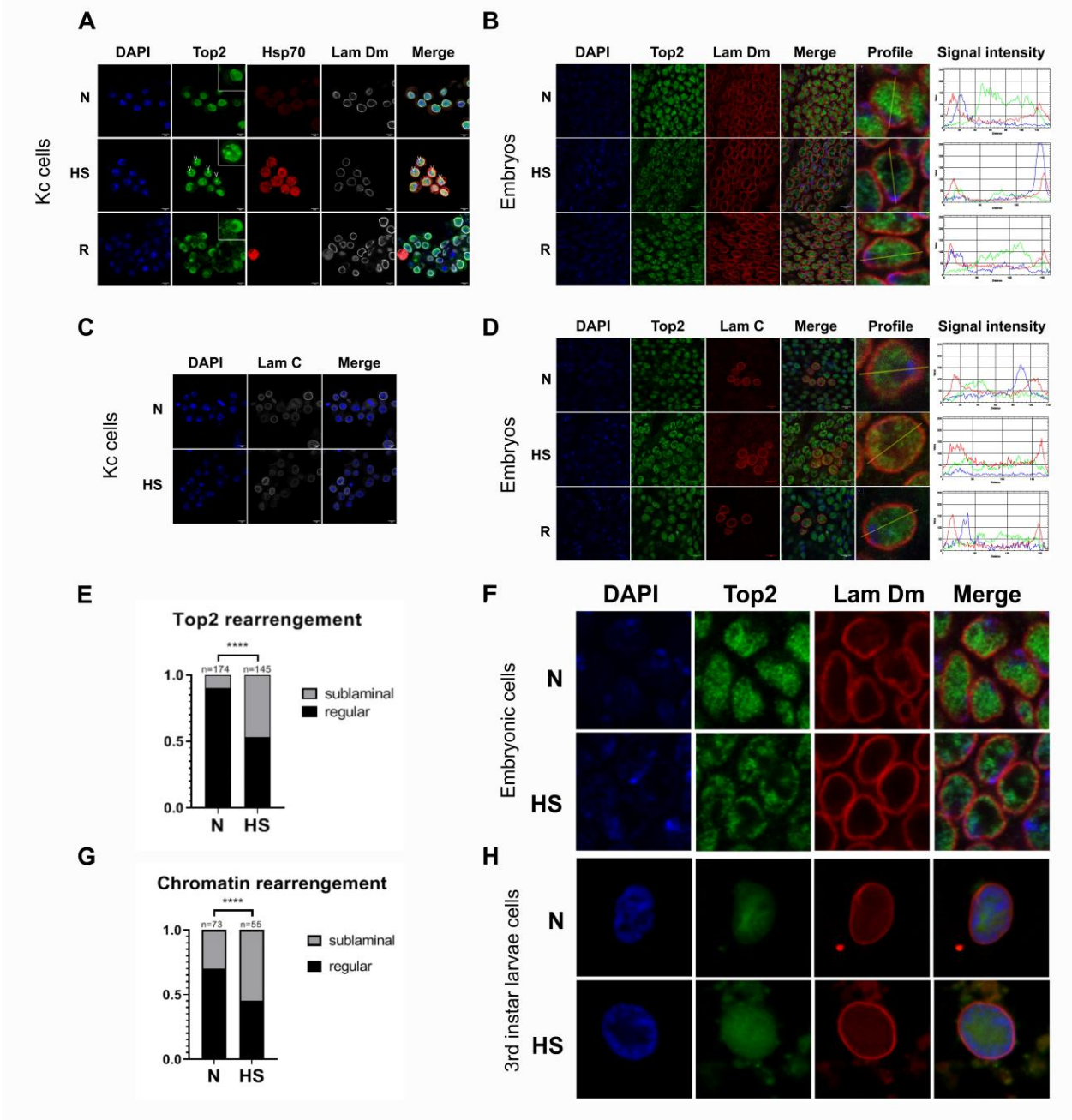
A
DAPI
Top2
Hsp70
Lam Dm
Merge
Kc cells
N
HS
R
B
DAPI
Top2
Lam Dm
Merge
Profile
Signal intensity
Embryos
N
HS
R
C
DAPI
Lam C
Merge
Kc cells
N
HS
D
DAPI
Top2
Lam C
Merge
Profile
Signal intensity
Embryos
N
HS
R
E
Top2 rearrengement
****
n=174
n=145
1.0
0.5
0.0
sublaminal
regular
N
HS
F
DAPI
Top2
Lam Dm
Merge
Embryonic cells
N
HS
G
Chromatin rearrengement
****
n=73
n=55
1.0
0.5
0.0
sublaminal
regular
N
HS
H
3rd instar larvae cells
N
HS

Figure 5

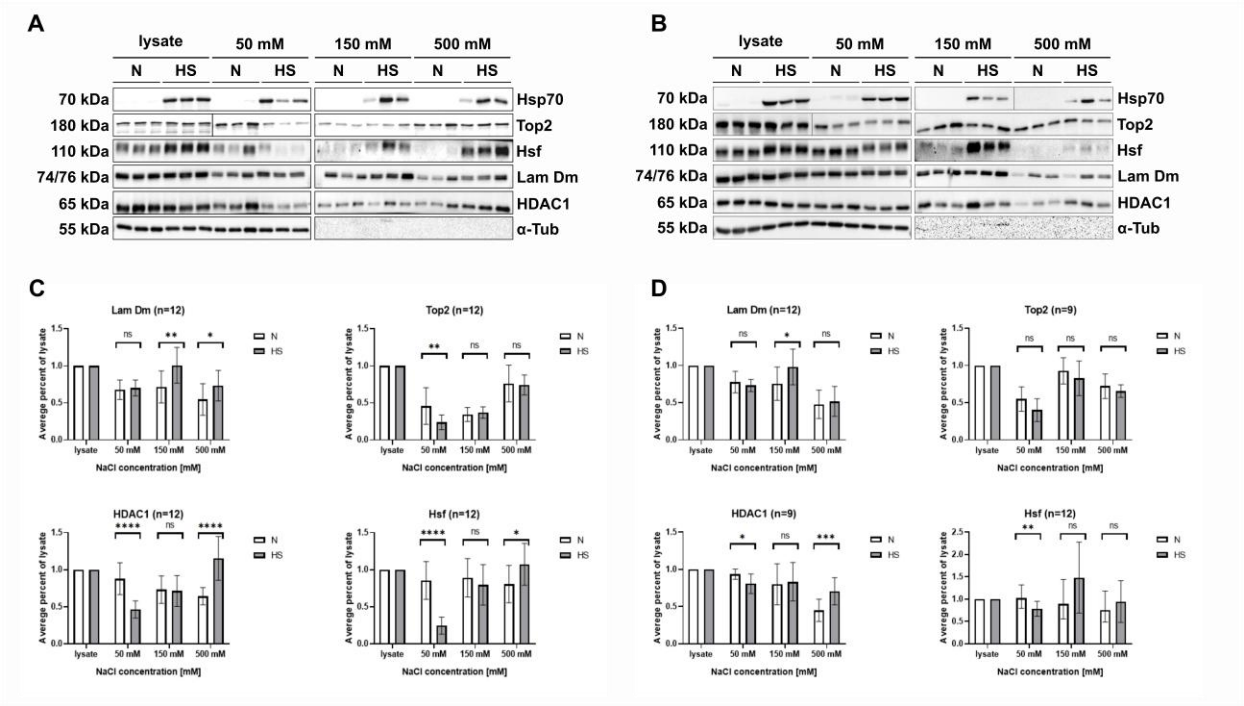
A
lysate
50 mM
150 mM
500 mM
N
HS
70 kDa
180 kDa
110 kDa
74/76 kDa
65 kDa
55 kDa
Hsp70
Top2
Hsf
Lam Dm
HDAC1
α-Tub
B
C
Lam Dm (n=12)
Top2 (n=12)
HDAC1 (n=12)
Hsf (n=12)
D
Lam Dm (n=12)
Top2 (n=9)
HDAC1 (n=9)
Hsf (n=12)
Average percent of lysate
NaCl concentration [mM]
ns
*
**
***
****

Figure 6

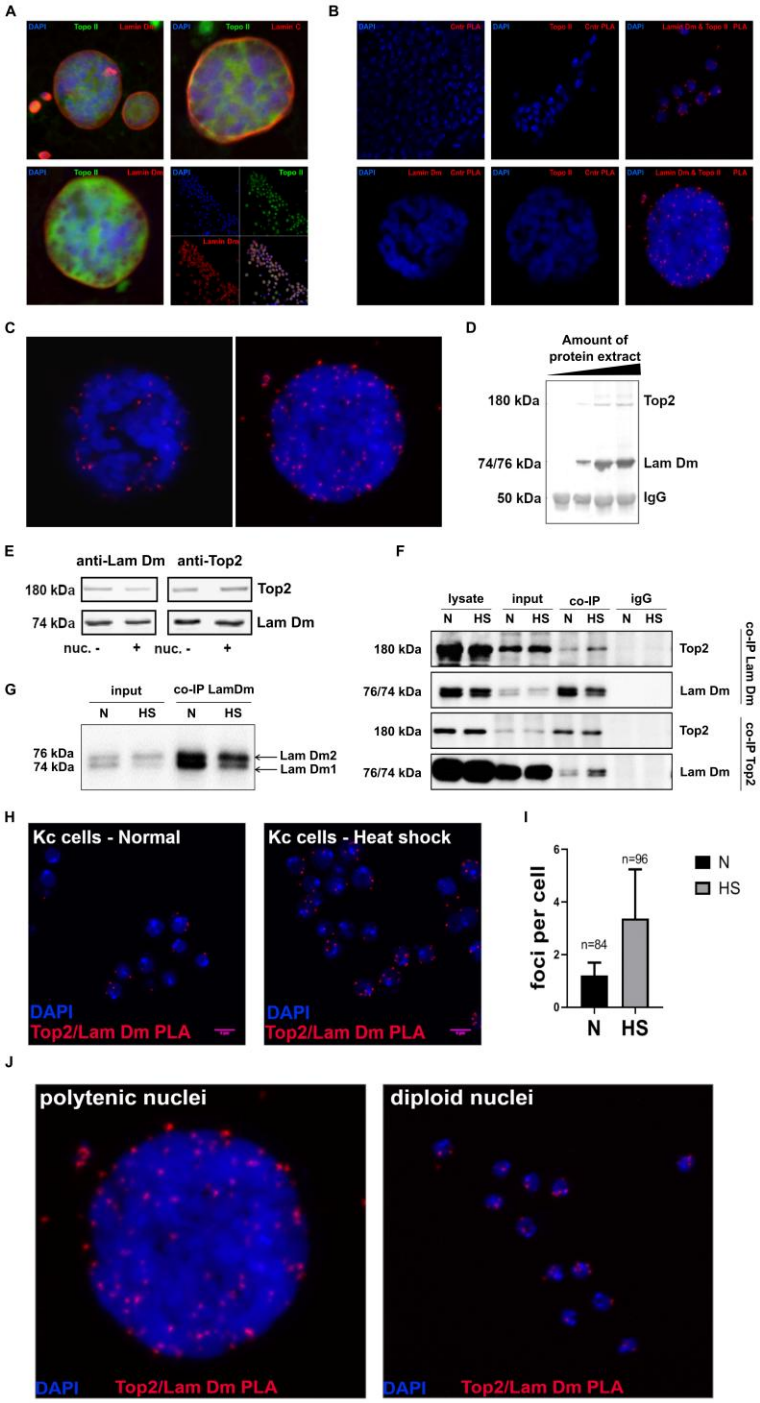
A
B
C
D
Amount of protein extract
180 kDa
Top2
74/76 kDa
Lam Dm
50 kDa
IgG
E
anti-Lam Dm
anti-Top2
180 kDa
Top2
74 kDa
Lam Dm
nuc. -
+
nuc. -
+
F
lysate
input
co-IP
igG
N
HS
N
HS
N
HS
N
HS
180 kDa
Top2
76/74 kDa
Lam Dm
co-IP Lam Dm
180 kDa
Top2
76/74 kDa
Lam Dm
co-IP Top2
G
input
co-IP LamDm
N
HS
N
HS
76 kDa
74 kDa
Lam Dm2
Lam Dm1
H
Kc cells - Normal
DAPI
Top2/Lam Dm PLA
Kc cells - Heat shock
DAPI
Top2/Lam Dm PLA
I
foci per cell
6
4
2
0
n=84
n=96
N
HS
N
HS
J
polytenic nuclei
DAPI
Top2/Lam Dm PLA
diploid nuclei
DAPI
Top2/Lam Dm PLA

Figure 7

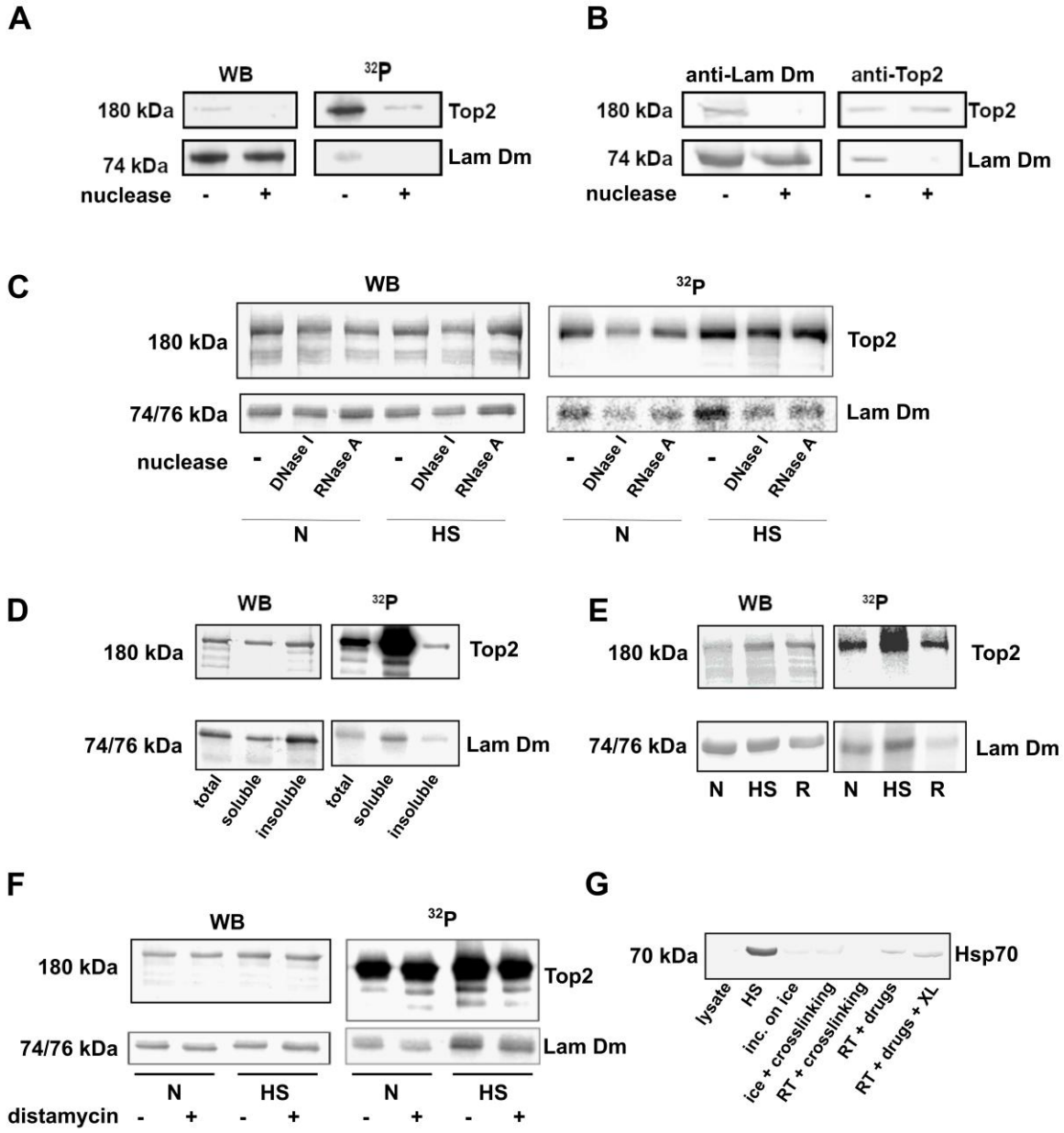
A
WB
32P
180 kDa
Top2
74 kDa
Lam Dm
nuclease
-
+
-
+
B
anti-Lam Dm
anti-Top2
180 kDa
Top2
74 kDa
Lam Dm
nuclease
-
+
-
+
C
WB
32P
180 kDa
Top2
74/76 kDa
Lam Dm
nuclease
-
DNase I
RNase A
-
DNase I
RNase A
-
DNase I
RNase A
-
DNase I
RNase A
N
HS
N
HS
D
WB
32P
180 kDa
Top2
74/76 kDa
Lam Dm
total
soluble
insoluble
total
soluble
insoluble
E
WB
32P
180 kDa
Top2
74/76 kDa
Lam Dm
N
HS
R
N
HS
R
F
WB
32P
180 kDa
Top2
74/76 kDa
Lam Dm
N
HS
N
HS
distamycin
-
+
-
+
-
+
-
+
G
70 kDa
Hsp70
lysate
HS
inc. on ice
ice + crosslinking
RT + crosslinking
RT + drugs
RT + drugs + XL

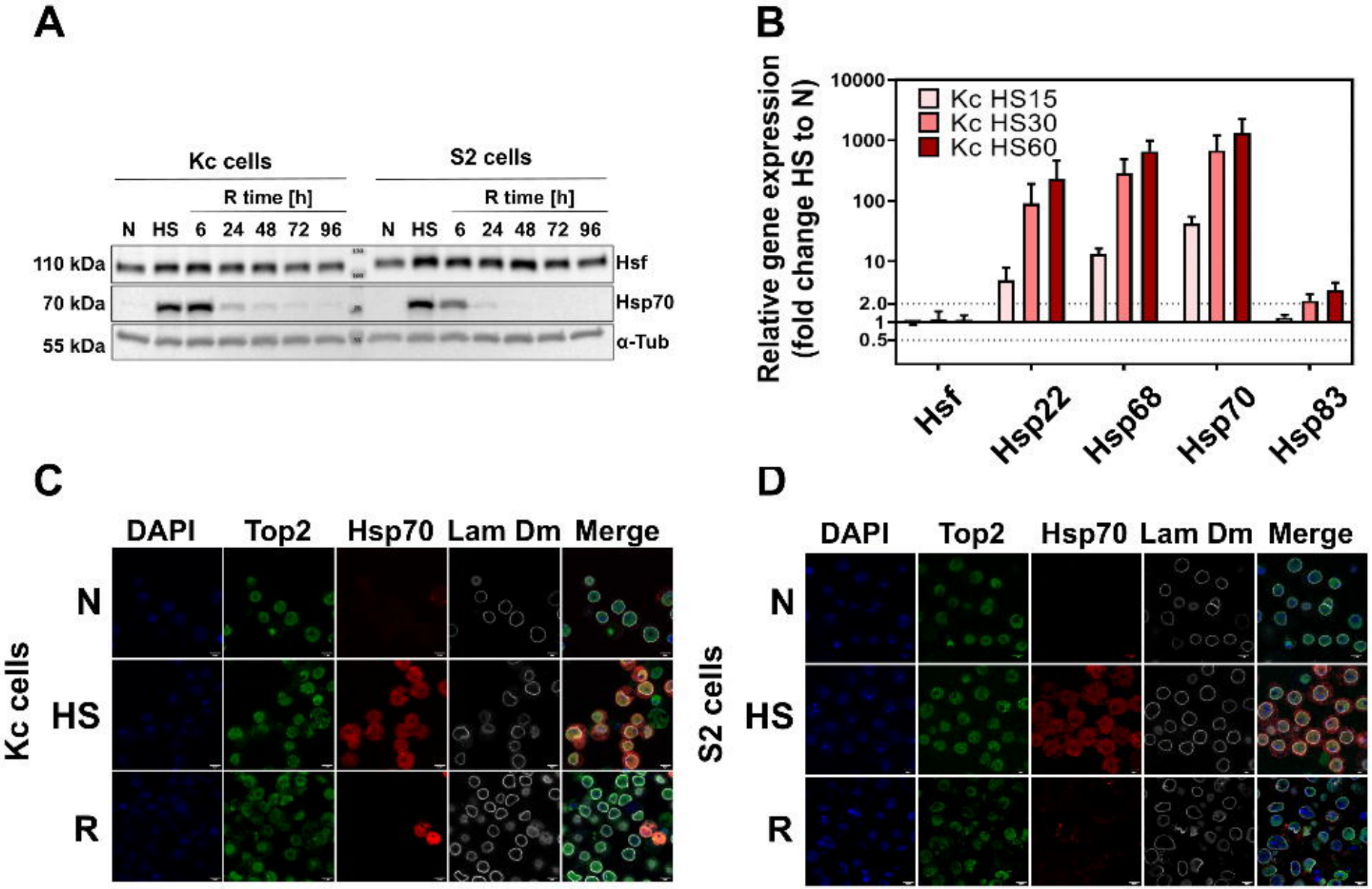
A
Kc cells
S2 cells
R time [h]
N HS 6 24 48 72 96
110 kDa
70 kDa
55 kDa
Hsf
Hsp70
α-Tub
B
Relative gene expression (fold change HS to N)
Kc HS15
Kc HS30
Kc HS60
10000
1000
100
10
2.0
1
0.5
Hsf
Hsp22
Hsp68
Hsp70
Hsp83
C
DAPI
Top2
Hsp70
Lam Dm
Merge
Kc cells
N
HS
R
D
S2 cells

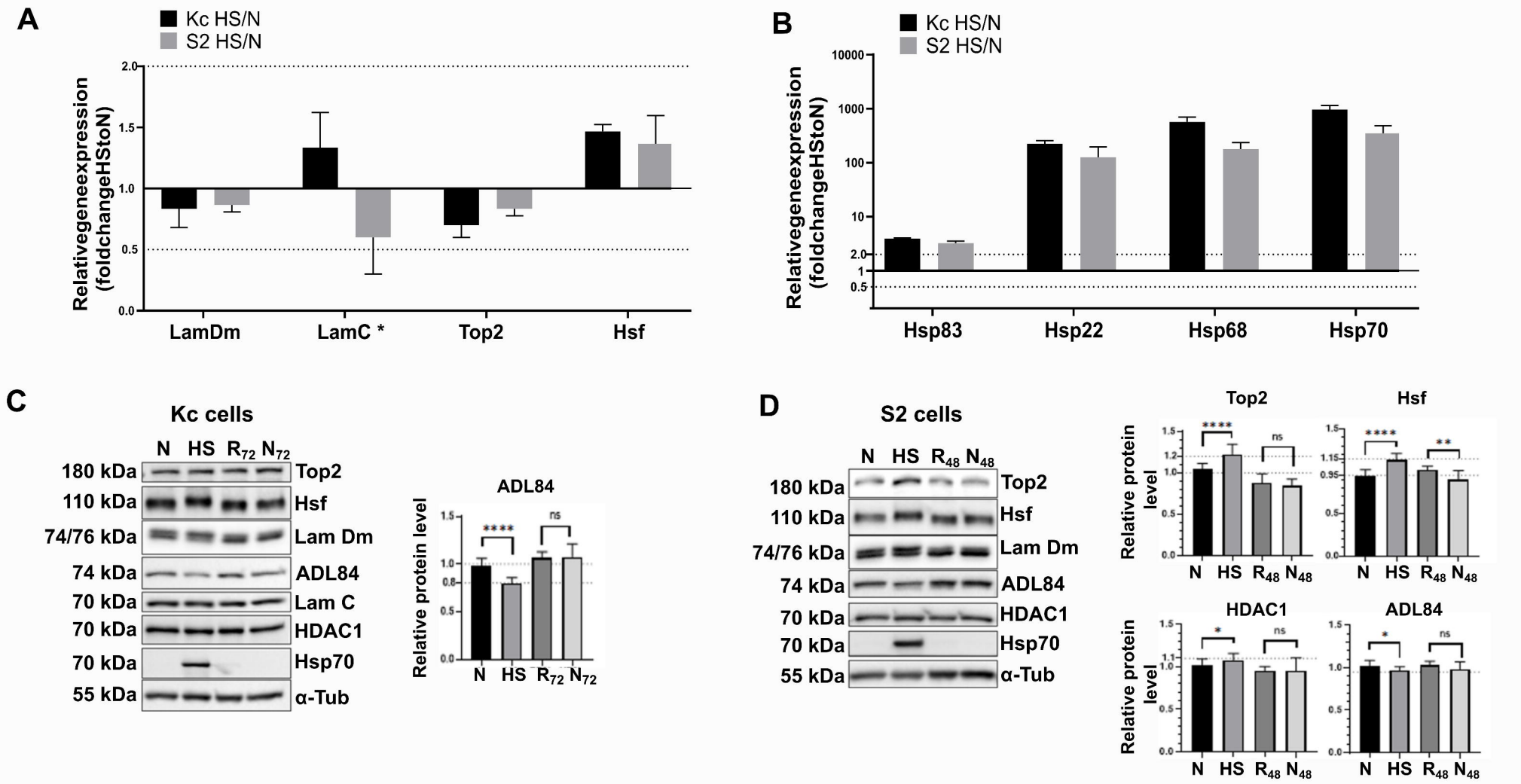
A
Kc HS/N
S2 HS/N
Relativegeneexpression (foldchangeHStoN)
2.0
1.5
1.0
0.5
0.0
LamDm
LamC *
Top2
Hsf
B
Kc HS/N
S2 HS/N
Relativegeneexpression (foldchangeHStoN)
10000
1000
100
10
2.0
1
0.5
Hsp83
Hsp22
Hsp68
Hsp70
C
Kc cells
N HS R72 N72
180 kDa Top2
110 kDa Hsf
74/76 kDa Lam Dm
74 kDa ADL84
70 kDa Lam C
70 kDa HDAC1
70 kDa Hsp70
55 kDa α-Tub
ADL84
Relative protein level
****
ns
N HS R72 N72
D
S2 cells
N HS R48 N48
180 kDa Top2
110 kDa Hsf
74/76 kDa Lam Dm
74 kDa ADL84
70 kDa HDAC1
70 kDa Hsp70
55 kDa α-Tub
Top2
Hsf
HDAC1
ADL84
Relative protein level
****
ns
**
*
N HS R48 N48

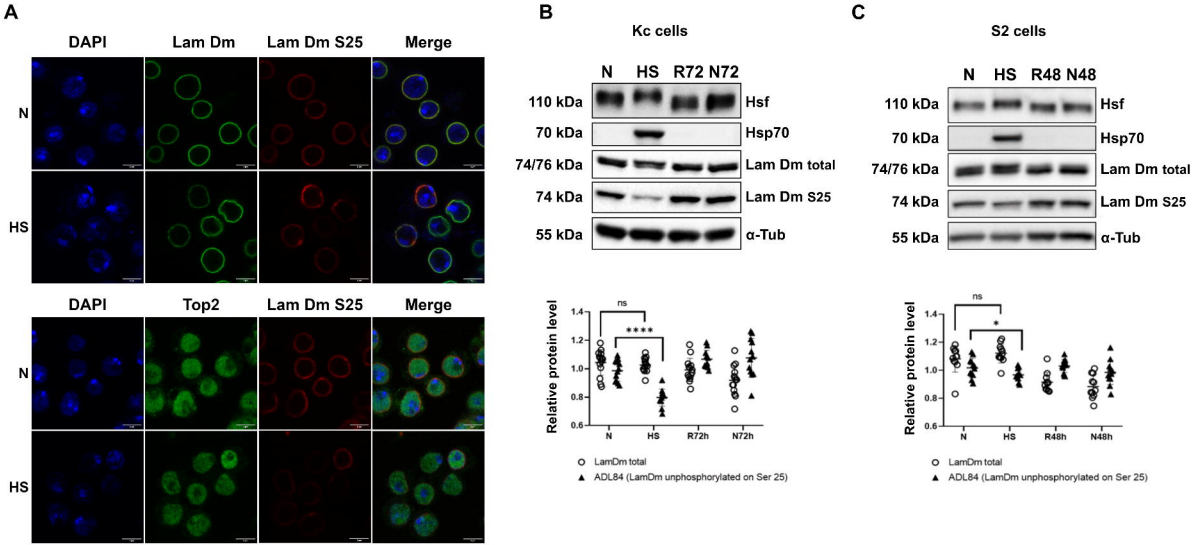
A
DAPI
Lam Dm
Lam Dm S25
Merge
N
HS
DAPI
Top2
Lam Dm S25
Merge
N
HS
B
Kc cells
N
HS
R72
N72
110 kDa
Hsf
70 kDa
Hsp70
74/76 kDa
Lam Dm total
74 kDa
Lam Dm S25
55 kDa
α-Tub
Relative protein level
ns
****
N
HS
R72h
N72h
LamDm total
ADL84 (LamDm unphosphorylated on Ser 25)
C
S2 cells
N
HS
R48
N48
110 kDa
Hsf
70 kDa
Hsp70
74/76 kDa
Lam Dm total
74 kDa
Lam Dm S25
55 kDa
α-Tub
Relative protein level
ns
*
N
HS
R48h
N48h
LamDm total
ADL84 (LamDm unphosphorylated on Ser 25)

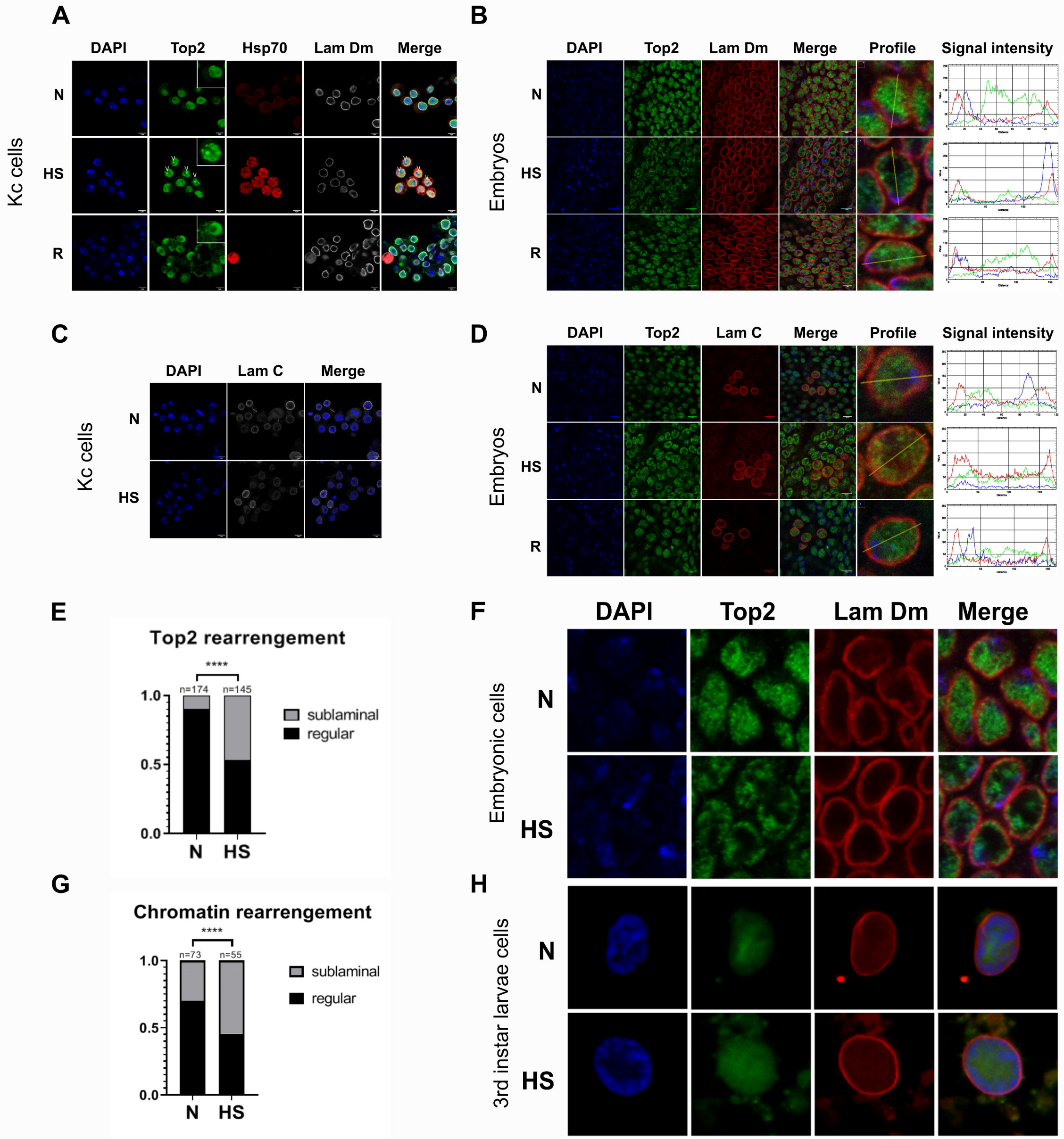
A
DAPI
Top2
Hsp70
Lam Dm
Merge
Kc cells
N
HS
R
B
DAPI
Top2
Lam Dm
Merge
Profile
Signal intensity
Embryos
N
HS
R
C
DAPI
Lam C
Merge
Kc cells
N
HS
D
DAPI
Top2
Lam C
Merge
Profile
Signal intensity
Embryos
N
HS
R
E
Top2 rearrengement
****
n=174
n=145
1.0
0.5
0.0
sublaminal
regular
N
HS
F
DAPI
Top2
Lam Dm
Merge
Embryonic cells
N
HS
G
Chromatin rearrengement
****
n=73
n=55
1.0
0.5
0.0
sublaminal
regular
N
HS
H
3rd instar larvae cells
N
HS

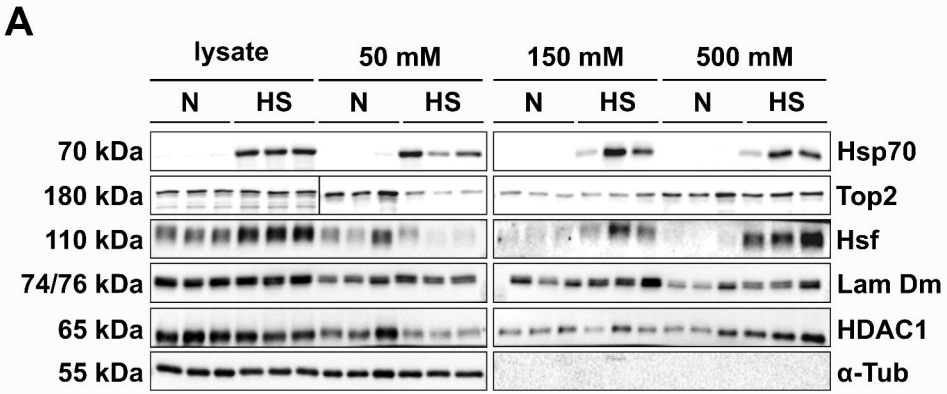
A
lysate
50 mM
150 mM
500 mM
N
HS
70 kDa
180 kDa
110 kDa
74/76 kDa
65 kDa
55 kDa
Hsp70
Top2
Hsf
Lam Dm
HDAC1
α-Tub

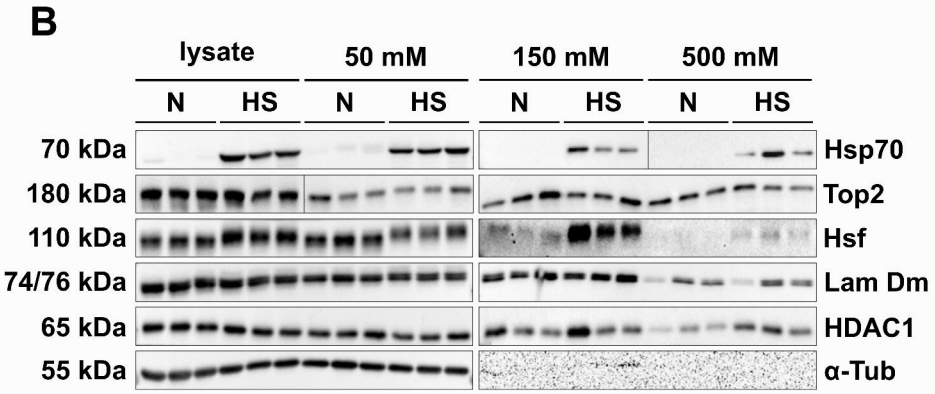
B
lysate
50 mM
150 mM
500 mM
N
HS
70 kDa
180 kDa
110 kDa
74/76 kDa
65 kDa
55 kDa
Hsp70
Top2
Hsf
Lam Dm
HDAC1
α-Tub

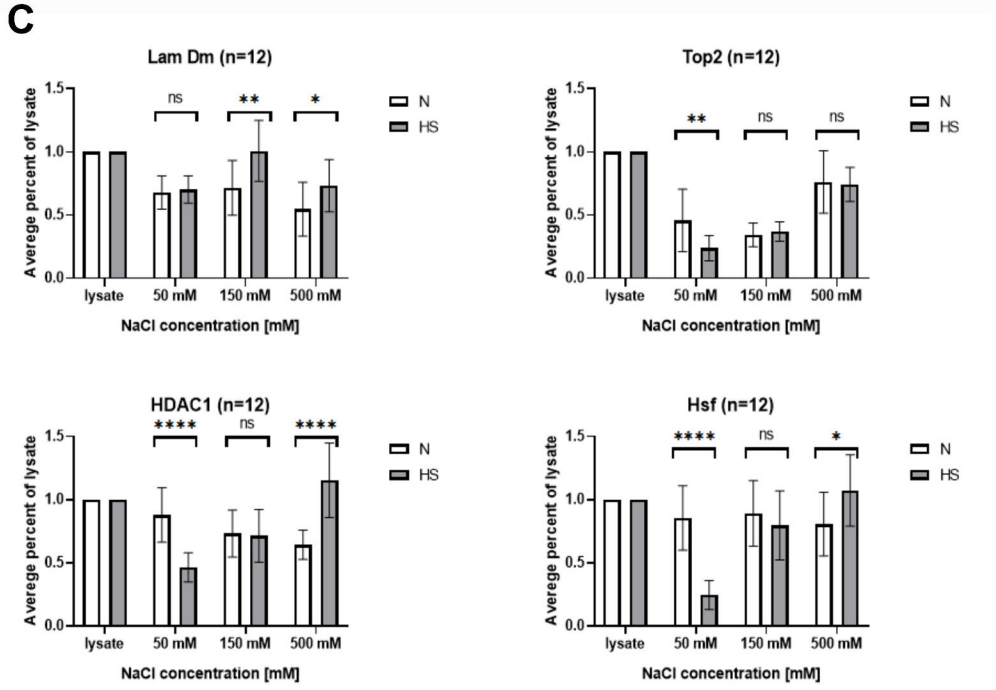
C
Lam Dm (n=12)
Top2 (n=12)
HDAC1 (n=12)
Hsf (n=12)
Averege percent of lysate
NaCl concentration [mM]
lysate
50 mM
150 mM
500 mM
N
HS
ns
*
**
****

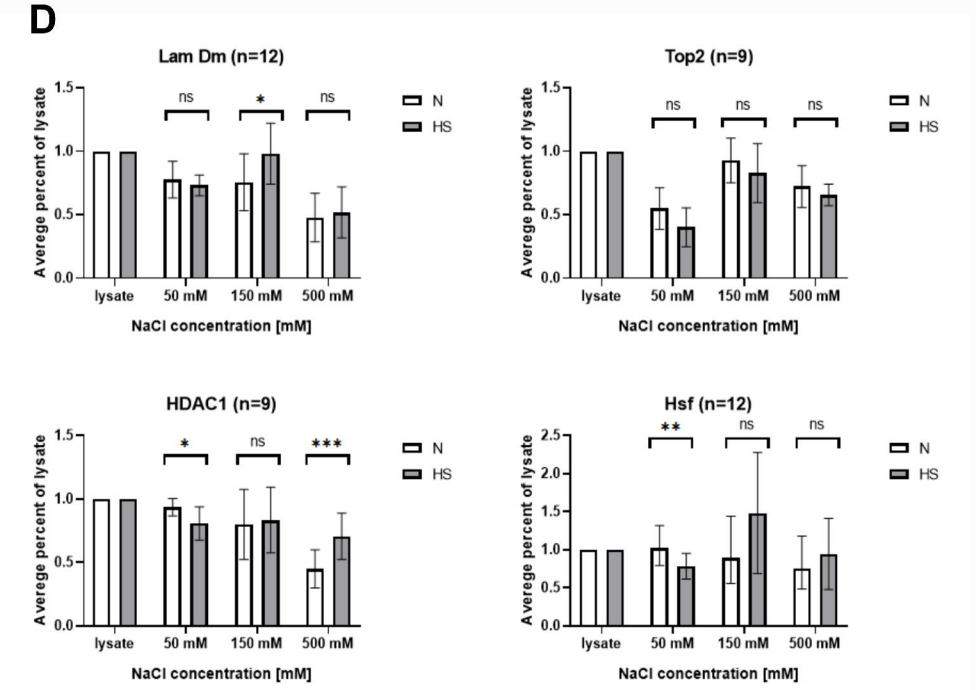
D
Lam Dm (n=12)
Top2 (n=9)
HDAC1 (n=9)
Hsf (n=12)
Averege percent of lysate
NaCl concentration [mM]
lysate
50 mM
150 mM
500 mM
N
HS
ns
*
**
***

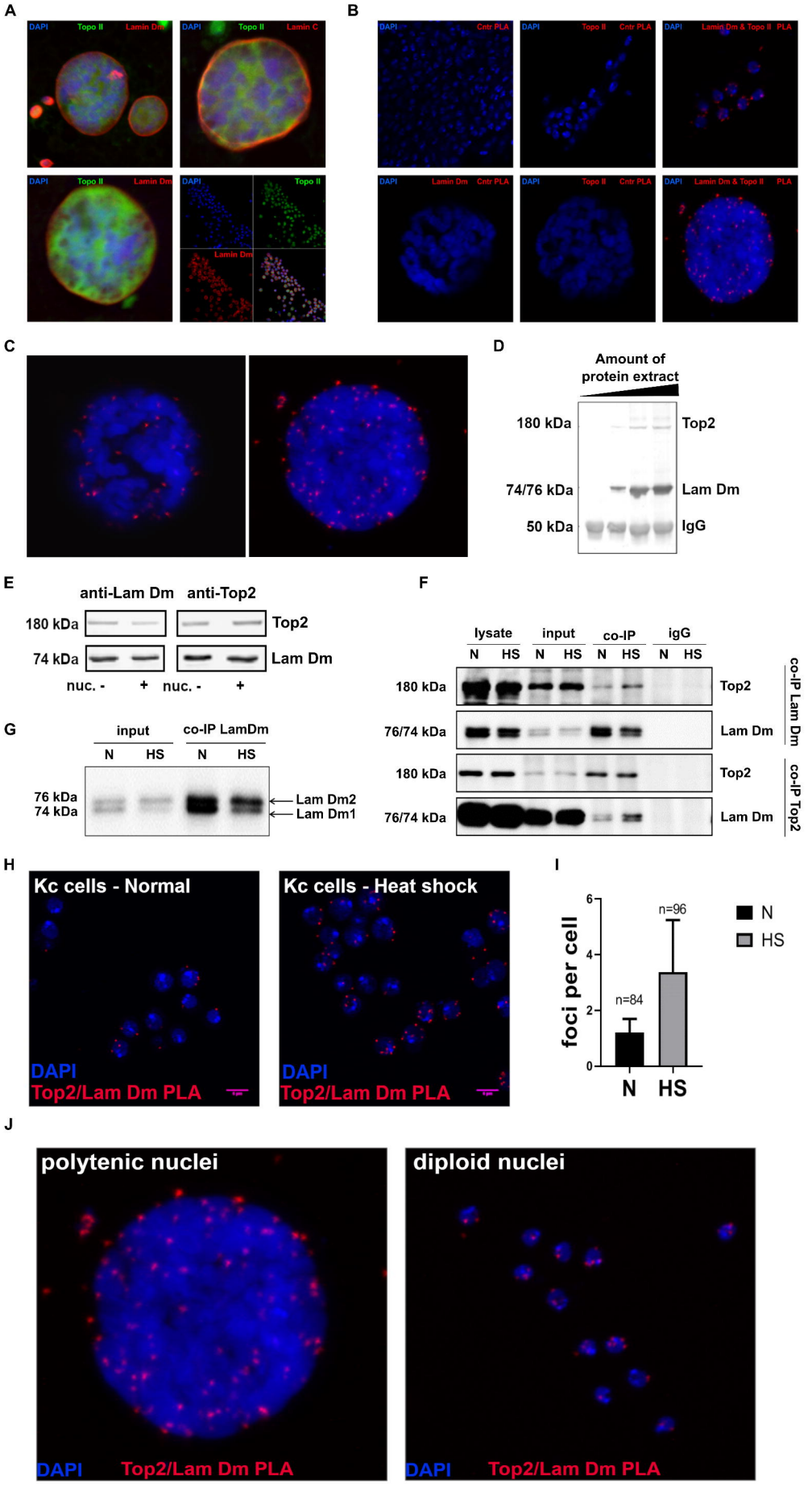
A
DAPI Topo II Lamin Dm
DAPI Topo II Lamin C
DAPI Topo II Lamin Dm
DAPI Topo II Lamin Dm
B
DAPI Cntr PLA
DAPI Topo II Cntr PLA
DAPI Lamin Dm & Topo II PLA
DAPI Lamin Dm Cntr PLA
DAPI Topo II Cntr PLA
DAPI Lamin Dm & Topo II PLA
C
D
Amount of protein extract
180 kDa Top2
74/76 kDa Lam Dm
50 kDa IgG
E
anti-Lam Dm anti-Top2
180 kDa Top2
74 kDa Lam Dm
nuc. - + nuc. - +
F
lysate input co-IP igG
N HS N HS N HS N HS
180 kDa Top2
76/74 kDa Lam Dm
co-IP Lam Dm
180 kDa Top2
76/74 kDa Lam Dm
co-IP Top2
G
input co-IP LamDm
N HS N HS
76 kDa
74 kDa
Lam Dm2
Lam Dm1
H
Kc cells - Normal
DAPI
Top2/Lam Dm PLA
Kc cells - Heat shock
DAPI
Top2/Lam Dm PLA
I
foci per cell
6
4
2
0
n=84
n=96
N
HS
N HS
J
polytenic nuclei
DAPI Top2/Lam Dm PLA
diploid nuclei
DAPI Top2/Lam Dm PLA

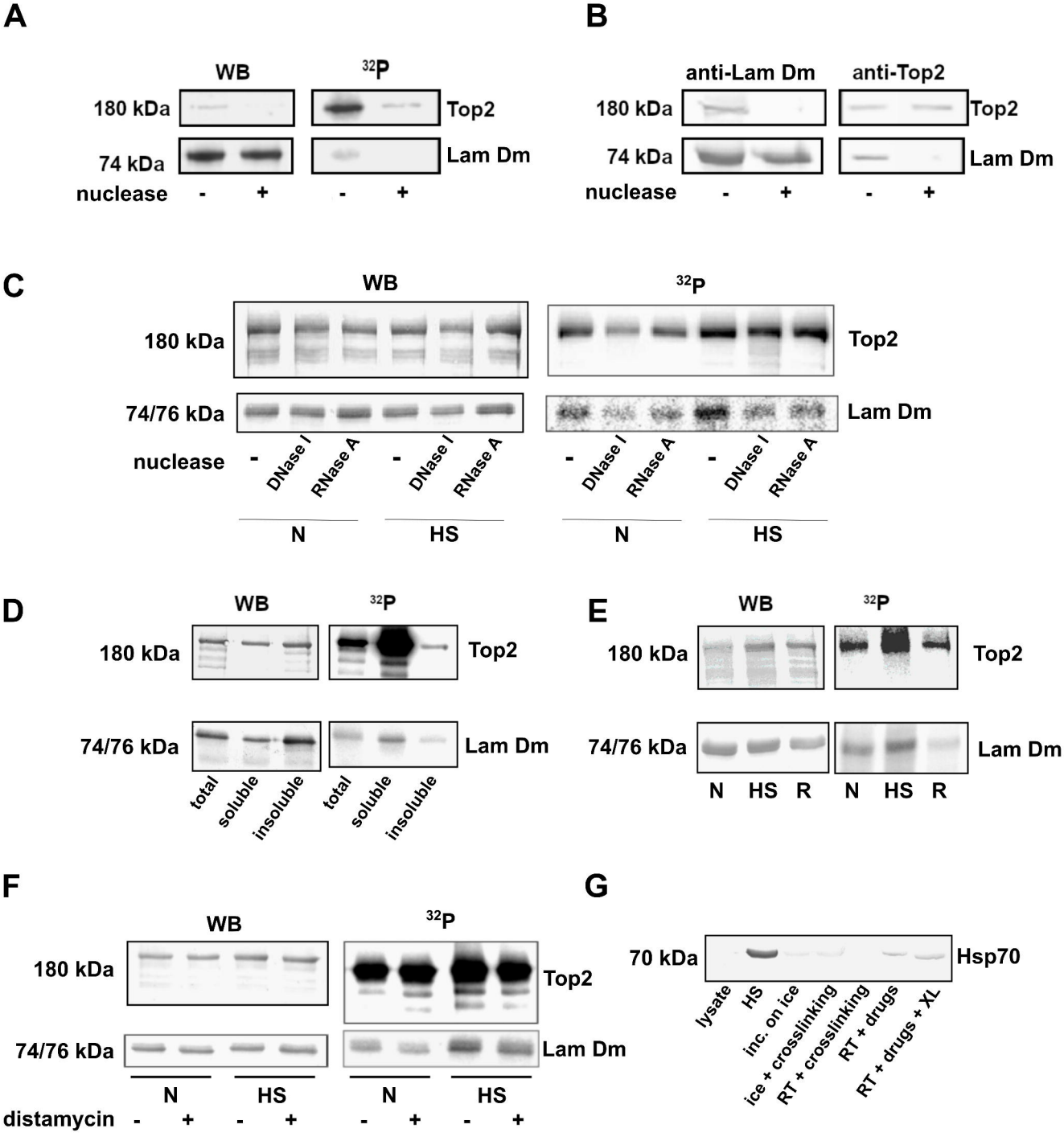
A
WB
32P
180 kDa
74 kDa
Top2
Lam Dm
nuclease
-
+
B
anti-Lam Dm
anti-Top2
C
74/76 kDa
DNase I
RNase A
N
HS
D
total
soluble
insoluble
E
R
F
distamycin
G
70 kDa
Hsp70
lysate
inc. on ice
ice + crosslinking
RT + crosslinking
RT + drugs
RT + drugs + XL